# AN ABSTRACT OF THE THESIS OF

Marian Jamieson for the degree of Master of Science in Civil Engineering presented on May 30, 2019.

Title: Investigation of Multi-constellation RTK GNSS Survey Productivity and Coordinate Accuracy

Abstract approved: _____

Michael J. Olsen

This study evaluates the productivity and accuracy of surveys completed with single-base real-time kinematic (RTK) Global Navigation Satellite Systems (GNSS) using four different GNSS constellation combinations: (1) GPS-only, (2) GPS+GLONASS, (3) GPS+Galileo+BeiDou, and (4) GPS+GLONASS+Galileo+BeiDou. For this comparison, we set up a test site consisting of 20 stations ranging with obstructions from low to severe conditions, primarily resulting from trees. Reference coordinates for each station were obtained through a least squares adjustment of total station and static GNSS observations. In the field surveys, we completed fourteen rounds of 30-second RTK occupations on each station across a period of five days in January 2019 using two antennas with a total of four receivers (two per antenna), each set to record a different constellation combination. Observations with the second antenna followed immediately behind the first antenna in order to maintain consistent satellite conditions for all constellation combinations. In comparison to the reference coordinates, we found that additional constellations dramatically improved productivity in the field, particularly in high obstruction conditions where the percent of fixed observations increased with each additional constellation from 15%, 21%, 70%, to 91%. However, the impact of additional constellations on accuracy is less clear from the data. GPS+GLONASS generally produced the smallest RMS values, despite larger bias. Combinations (3) and (4) produced solutions with smaller biases but larger standard deviations as compared to GPS+GLONASS.

# Investigation of Multi-constellation RTK GNSS Survey Productivity and Coordinate Accuracy

by
Marian Jamieson

A THESIS

submitted to

Oregon State University

in partial fulfillment of
the requirements for the
degree of

Master of Science

Presented May 30, 2019
Commencement June 2019

Master of Science thesis of Marian Jamieson presented on May 30, 2019

APPROVED:

Major Professor, representing Civil Engineering

Head of the School of Civil and Construction Engineering

Dean of the Graduate School

I understand that my thesis will become part of the permanent collection of Oregon State University libraries. My signature below authorizes release of my thesis to any reader upon request.

Marian Jamieson, Author

# ACKNOWLEDGEMENTS

I would first like to thank Eric Stalker for helping with RTK data collection, life, and always asking “how can I help.” I appreciate the support of my thesis advisor, Dr. Michael Olsen, for the continuous advice, patience, and encouragement. Eric Gakstatter of Discovery Management Group inspired me to pursue this topic as well as provided RTK equipment, financial assistance, and general support. Mark Armstrong assisted Discovery Management Group with setting up the RTK base used in this study. I am grateful for the financial support provided by Oregon State University and the Oregon Department of Transportation for my graduate studies. Leica Geosystems, Microsurvey, and David Evans & Associates provided most of the survey hardware for the ground truth surveys and some of the software for analysis. Dr. Farid Javadnejad graciously developed and ran Skyplotter for this research. Lastly, I appreciate Dr. Dan Gillins and Mike Eddy for mentoring me as an undergraduate research assistant and sparking a passion for geomatics.

# TABLE OF CONTENTS

Page

# LIST OF FIGURES

Figure Page

# LIST OF TABLES

## 1. Introduction

GNSS (Global Navigation Satellite Systems) is an invaluable tool in positioning for engineering surveys and many other applications. Real-time kinematic (RTK) GNSS provides corrections to achieve precise coordinates in real time directly in the field. RTK uses a base station consisting of a GNSS receiver setup at a known position to broadcast corrections to the rover receiver located at a point of interest to be surveyed. In GPS-only single-base RTK surveying, five satellites are required to resolve the unknowns and initialize the survey. While adequate satellite availability is not as difficult to achieve as it was in the early days of civilian GPS, situations such as surveying in locations with obstructions such as urban centers, canyons, or forests can still be challenging with limited visible satellites.

GNSS constellations are growing quickly. The U.S. GPS has maintained a full constellation since 1995. GLONASS (GLO), developed by Russia, reached a full constellation in 1995, experienced a decline in availability, and then has maintained a full constellation since 2011. Various regional systems have been developed, but it was not until 2011 when Galileo (GAL, European) and BeiDou Navigation Satellite System (BDS, Chinese) first launched satellites for global systems. In June 2019, Galileo and BeiDou have 22 and 21 globally operational satellites, respectively (in addition to the 12 regionally operational BDS satellites). Both systems intend to have full constellations by 2020.

Because the global availability of these systems have only recently become operational, there are few published works evaluating multi-constellation GNSS beyond GPS+GLO, particularly within the North American Region. Most of the available studies considering 3+ constellations evaluate precision not accuracy, locations only with minimal to low obstruction, or data collected before constellations were globally accessible with a sufficient number of satellites (i.e., these studies used the regional satellites).

The primary objective of this study is to evaluate the impacts of multi-constellation RTK GNSS under varying overhead conditions, from low to severe obstruction under forested conditions at a site in North America where these systems have only been available for a short time. To achieve this objective, we compare different GNSS constellation combinations and quantify the (1) improvements in survey productivity, (2) influence on coordinate accuracy, and (3) validity of receiver-estimated precision.

To achieve these research objectives, a test site was established in the western United States at nearly 45° north latitude. The site consists of 20 stations under a variety of obstruction conditions up to 87.5% obstructed sky, predominately resulting from evergreen and deciduous trees. The single-base RTK GNSS survey compared four constellation combinations (Table 1): (1) GPS-only, (2) GPS+GLO, (3) GPS+GAL+BDS, and (4) GPS+GLO+GAL+BDS. Observations under each combination were completed within minutes of one another to ensure that observed differences did not result from significantly different satellite configurations.

Table 1. Constellation combinations used in RTK testing.

| Number of Constellations | GPS | GLONASS (GLO) | Galileo (GAL) | BeiDou (BDS) |
|---|---|---|---|---|
| **4** | X | X | X | X |
| **3** | X | | X | X |
| **2** | X | X | | |
| **1** | X | | | |

In order to investigate survey productivity with the different combinations, we evaluated the proportion of epochs with fixed integer ambiguity compared with total epochs, where an epoch is each one second observation. In order to assess coordinate accuracy, we derived reference coordinates from a least squares adjustment of static GNSS and total station observations. The reference coordinates were differenced from each epoch of RTK survey coordinates to estimate accuracy of each observation. These estimated accuracies were then compared to receiver-estimated

precisions, which many GNSS users (and some manufacturers) mistake as a measure of estimated accuracy.

## 2. Background

GNSS is useful for positioning at a global scale; however, local corrections are required to achieve accurate and precise coordinates. GNSS observations can be collected using static or kinematic positioning techniques. Systematic errors such as clock differences and atmospheric effects in the ionosphere and troposphere affect the travel time between the satellites and the rover and thus affect the quality of positioning. These observations can be corrected using relative positioning or precise point positioning (PPP) techniques as well as others that are less relevant to this study. Static GNSS positioning typically requires 20 minute to multiple-hour occupations and post-processing to achieve desired precision. Post-processing utilizes relative positioning or precise point positioning to achieve cm- to mm-level precision (Jamieson and Gillins 2018; Van Sickle 2015) in the resulting coordinates. GPS-only static observations require a minimum of 4 satellites to resolve unknowns. To implement other configurations, one to two additional satellites per additional constellation are needed to resolve unknowns and clock biases without introducing additional assumptions. Each manufacturer handles the additional satellites in the final solution with different techniques.

Kinematic GNSS positioning can be corrected in real time as well as through post-processing methods if the individual satellite observations are logged (e.g., RINEX file). RTK GNSS ordinarily consists of occupations ranging from 1 second to 10 minutes in durations, with relative positioning corrections obtained in real-time from a base station setup at a known point (single-base). RTK can also be completed within a network, where corrections are interpolated from a network of permanent, continuously operating base stations. PPP techniques can also be applied in real time to kinematic GNSS positioning (Van Sickle 2015). In relative positioning corrections

are computed based on correcting the observed positions of the base to its known position; whereas, in PPP corrections are computed entirely by modeling from a network of reference stations. Although PPP is being utilized more and more and the subject of much current research, it substantially less popular compared with RTK in the surveying engineering community.

Network RTK is generally more accurate and precise than single-base RTK (Allahyari et al. 2018; Weaver et al. 2018). However, many real time networks have not yet made multi-GNSS available, including within our study area. In June 2019, only 90% of the local Oregon Real-time GNSS Network (ORGN) base stations have GLONASS enabled (Oregon Department of Transportation 2018) in addition to GPS; however, Galileo and BeiDou are not available within this network. As a result, single-base RTK was requisite for this study. As a result, a key motivation behind this study was to help inform network RTK providers such as the ORGN if offering multi-constellation corrections beyond GPS+GLO would be worth pursuing further, given the financial implications associated with upgrades.

As stated previously, in GPS-only single-base RTK, five satellites are required to resolve the unknowns and achieve a solution with fixed integer ambiguities, herein termed a “fixed solution.” One to two additional satellites per additional GNSS constellation are needed for a multi-GNSS survey. In other words, without introducing additional assumptions, a minimum of eight satellites are required to resolve unknowns in the case of four-constellation RTK. Nowadays, this quantity of satellites is readily achievable in low obstruction conditions, but becomes more difficult under higher obstruction in forested or urban environments (Van Sickle 2015).

Fortunately, as more GNSS approach full global constellations, many more satellites are available (Figure 1), which improves satellite geometry. Both the United States

GPS and Russian GLONASS reached full constellations in 1995. GPS has maintained a constellation of approximately 31 satellites since that time. GLONASS experienced a decline in availability, but has maintained a constellation of about 24 satellites since 2011. Regional systems include the Japanese QZSS, Indian IRNSS/NavIC, and Chinese Compass (now part of BeiDou). In 2011, the European Union Galileo and the Chinese BeiDou first launched satellites with the intent to reach full constellations by 2020. Galileo has added 14 satellites since 2015 to reach a total of 22 currently available satellites. BeiDou has added 18 globally orbiting satellites since 2016, reaching a total of 21 currently available globally orbiting satellites. These numbers do not include the 12 regionally available BeiDou satellites. Figure 1 shows the number of globally orbiting satellites versus their launch date, including only satellites operational at the time of writing. Note that satellites require months to years for testing before they are available for civilian use. For context, the total number of available satellites during the survey completed in this study from the four constellations ranged from 22 to 34, with a minimum of 7 available GPS satellites.

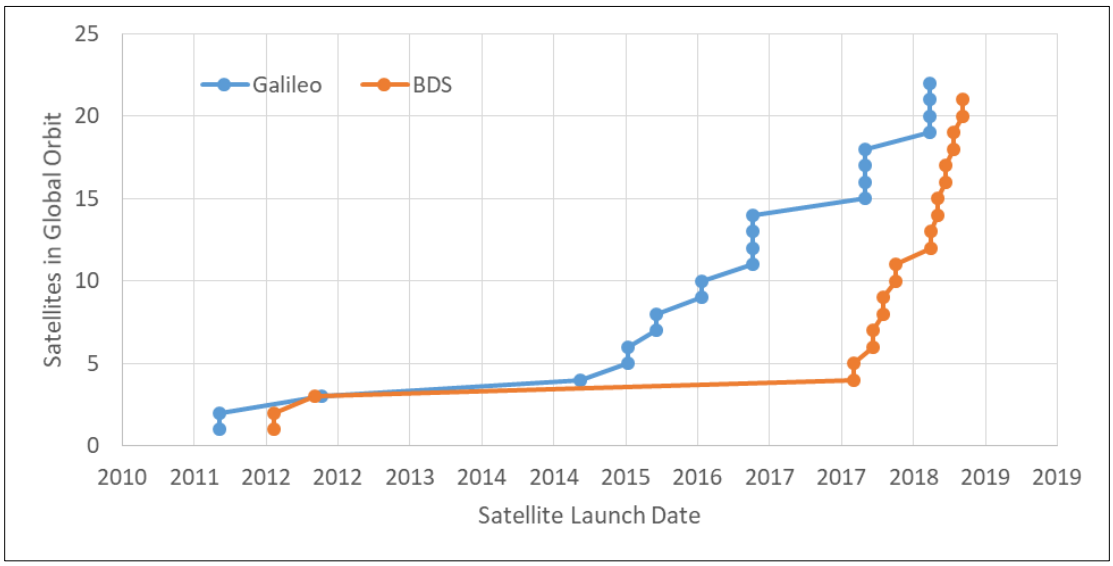


Figure 1. Galileo and BeiDou number of satellites in global orbits over time, including only satellites operational at the time of writing.

### *2.1 Previous Efforts Evaluating Multi-Constellation GNSS*

To date, there are several studies investigating the addition of GLONASS to GPS using different techniques to support varying applications. However, there are limited studies available that investigate field performance of three or more constellations on a global scale, mostly because the systems have not been available until recently in many locales (e.g., North America). Notably, there are published studies that evaluate results of three constellations in the Asia-Pacific region due to relatively long-term regional availability of BeiDou. The following section briefly summarizes those studies that are most comparable to our objectives.

Jamieson and Gillins (2018) evaluated post-processing static observations of durations 2 to 10 hours with GPS-only and GPS+GLO. The investigators found the addition of GLONASS reduced horizontal and vertical RMS values in the majority of, but not all, cases. Overall, the addition of GLONASS reduced horizontal RMS values by 17% and 36% in minimal and moderate multipathing environments, respectively. However, post-processing static occupations of 2 to 10 hours in duration can be less sensitive to multipath as the satellite geometries change throughout the observations. In real-time GNSS, occupations are short in duration and would have effectively the same constellation throughout the occupation. Further, RTK data is limited in reprocessing should an error occur. Redundant observations are often necessary to identify bad coordinates, which can reduce the efficiency of the field survey.

Generally, in a dual-frequency network RTK GNSS survey, the addition of GLONASS satellites has been found to significantly improve fixed solution availability (i.e. survey productivity) and only slightly improve solution accuracy/precision (Allahyari et al. 2018; Penna et al. 2012). Similarly, Weaver et al. (2018) found RTK network vertical accuracies improved 19% with the addition of GLONASS observables to GPS-only, in locales in the United States. Alternatively,

Martin and McGovern (2012) observed no significant difference were observed with the addition of GLONASS observables to network RTK from their study completed in Ireland.

Studies using regionally available BeiDou satellites for single-base RTK surveys have found improvements to solution fix rates and position precision when used in addition to GPS (Deng et al. 2014; Msaewe et al. 2017; Xi et al. 2018). Xi et al. (2018) specifically found that the addition of BeiDou to GPS improved precision by 20-30%. Li et al. (2015) presented a four-constellation real-time precise point positioning model using GPS, GLONASS, Galileo, and BeiDou (regional and global). They tested the model and found the four-constellation scenario to reduce time-to-fix by 70% and improve accuracy by 25% as compared to GPS-only.

Odolinski et al. (2015) evaluated single-frequency, single-baseline RTK using GPS, Galileo, BeiDou, and QZSS in Australia. The investigators used high cut off angles up to 40° to simulate urban canyons. They found that the additional constellations significantly reduced the time to obtain a fixed solution, allowed the use of higher cutoff angles, and improved coordinate precision. Additionally, the investigators noted that while correctly fixed positions have errors at the millimeter-centimeter level, incorrectly fixed positions can have errors at the decimeter-meter level that can be significantly worse than float solutions. Odolinski and Denys (2015) found similar results in New Zealand using multi-frequency single-baseline RTK with GPS, Galileo, BeiDou, and QZSS up to 25° elevation cut-off angles.

In a network RTK GNSS survey, Penna et al. (2012) found receiver estimated coordinate quality to generally correspond to actual accuracy, but GPS+GLONASS coordinate quality values were slightly optimistic compared to those from GPS-only. They observed marks under a variety of overhead conditions in an urban area, ranging

from low obstruction to urban canyon using survey-grade receivers from well-established manufacturers popular among traditional surveyors.

This study expands upon these prior works by focusing on globally available satellites and working under severe levels of natural obstructions, with short, single baseline RTK at roughly 45° north latitude in North America. Notably, many of the above studies occur in urban areas or areas with minimal to low obstruction. This study determines if these findings of improved survey productivity and coordinate accuracy remain true at higher levels of obstruction and within North America. Another unique aspect to this research is the use of two receivers to one antenna, enabling a more efficient survey to directly compare constellations with consistent satellite geometry. While splitting the antenna signal inevitably results in some signal loss, each receiver is impacted similarly; hence, the raw accuracy may be slightly impacted, but the comparison of accuracies is still valid. The receivers used in this study are popular within the GIS community and advertised as survey-grade but have not been widely tested within the surveying community. Lastly, studies performing extensive field surveys with 3+ constellations under different obstruction conditions are generally published between 2012 and 2015; however, many satellites have been added to Galileo and BeiDou since that time.

## 3. Test Site

We set up a test site in Western Oregon comprised of 20 stations relatively closely spaced within an approximate area of 220 m x 90 m (20,000 $m^2$). Although relatively small in area, the degree of obstruction varies substantially across the site. The stations consisted of predominately survey magnails set in tree roots and sidewalks under a wide range of obstruction conditions. The obstructions occur predominantly from trees, consisting of evergreen and deciduous trees of various sizes. Stations were numbered based on the order of acquisition during RTK GNSS data collection, approximately counter-clockwise.

Figure 2 provides a map of the site showing the stations identified by their obstruction category. Note that the satellite imagery in Figure 2 contains more vegetation than was present during RTK data collection given that the survey was completed in the winter months during leaf off conditions. However, because Stations 3, 12, 13, and 14 are predominantly obstructed by evergreen trees, the conditions at those stations would be more consistent with the base photograph. For other stations, the obstructions typically result from deciduous trees, so they would be expected to have fewer obstructions compared with the base photograph.


Figure 2. Map of project site, with stations identified by obstruction category.

### *3.1 Characterizing Obstructions*

Zenith photographs were acquired during the same week of the RTK survey (leaf-off conditions) to characterize the magnitude of obstruction at each station. To capture

these photographs, a digital SLR camera with a fisheye lens was attached to a 2-m fixed height pole using a custom mount (e.g., Figure 3). The 2-m pole was rotated so the top of the photograph would point at approximately true north, and the lens focus was set to infinity.

Figure 3. Obstruction photo occupying Station 3.

We analyzed each zenith photograph using *Skyplotter*, a custom Java application, which creates visibility plots by correcting the distorted fisheye photo, drawing concentric circles to show vertical angle (from horizon to zenith in 15° increments), and drawing azimuth lines at 30° increments. *Skyplotter* also calculates the percent of open sky within a hemispherical photograph from the point of observation from each station. Next, the stations were classified by percent of sky obstructed based on natural groupings. This resulted in four categories: low (<50%), moderate (56-62%), high (68-75%), and severe (>78%). The resulting visibility plots are shown in Figures

4 through 7, grouped by obstruction category. It should be noted that we found that *SkyPlotter* erroneously classified some cloud cover as obstruction under the default settings used, increasing the percent obstruction at low and moderate obstruction stations in an absolute sense. However, all of the photographs were captured within a 1-hour period, so cloud cover conditions were more or less consistent between stations.

While the estimate of percent of obstructions cannot fully capture the actual field conditions in an absolute sense, it does provide a relative representative metric for grouping stations by visibility at the stations. Other factors, such as the satellite geometry at the time of survey, play an important role in satellite availability. As an example, Stations 6 and 15 have similar percentages of obstructed sky, but notably different conditions in the field. Station 6 is located approximately 1 meter from a tree and has obstructions directly overhead. In contrast, Station 15 is about 5 meters from the nearest tree, has open sky directly overhead and has obstructions concentrated mostly to the side. Further, as will be shown later, the classification system based on the visibility plots was consistent with field observations of obstruction and its effect on the productivity of the survey, which is evidenced by the percent of fixed epochs obtained at the stations.

Low obstruction stations (Figure 4) have a percent of obstructed sky less than 50% and posed little to no difficulty in achieving a fixed solution for all constellation combinations. Although classified as low obstruction, Stations 1, 19, and 20 were more susceptible to multipath compared to the other stations due to vehicles parking nearby. Additionally, Station 20 is located close to a small deciduous tree that extends over the top of the station. That being said, the RTK survey field crew did not notice any reduction in fixed solutions at these stations as compared to other low obstruction stations. Subsequently, Stations 1, 19, and 20 were left grouped within the low obstruction category.

Moderate obstruction stations (Figure 5) have a percent of obstructed sky between 56% and 61% and showed some difficulties with achieving a fixed solution for the GPS-only configuration; however, other constellation combinations regularly achieved a fixed solution. High obstruction stations (Figure 6) have percent of obstructed sky between 68% and 74% and posed difficulty for all constellation combinations; however, every combination achieved a fixed solution at each of these stations at some point during the survey. Severely obstructed stations (Figure 7) have a percent of obstructed sky greater than 79%. At severely obstructed stations, a fixed solution was extremely difficult to obtain for any constellation combination; GPS-only (1) and GPS+GLO (2) achieved only one and two fixed occupations respectively on any of the severely obstructed stations.

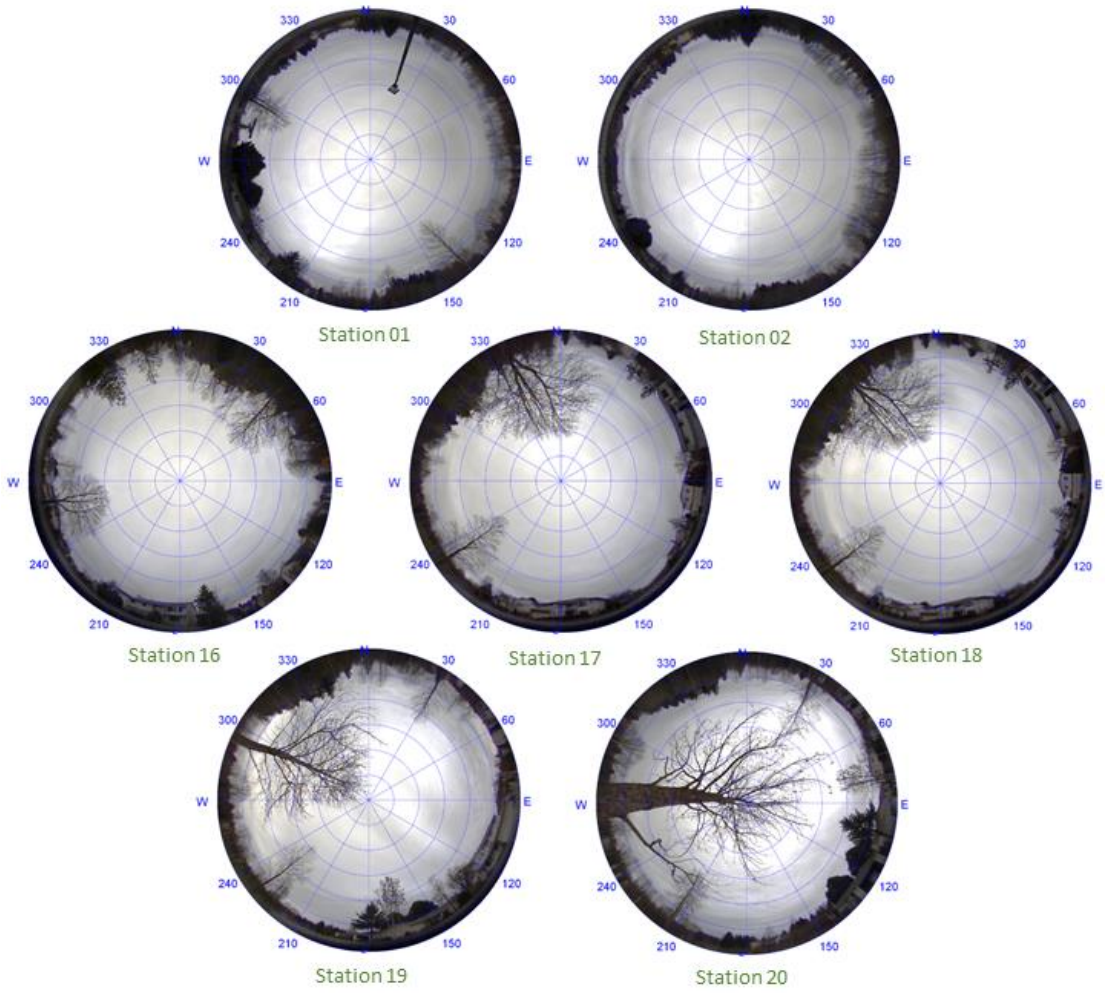


Figure 4. Hemispherical visibility plots of stations with low obstructions. The circles shown are 15° vertical angle increments from the top of the fixed height tripod on each station.

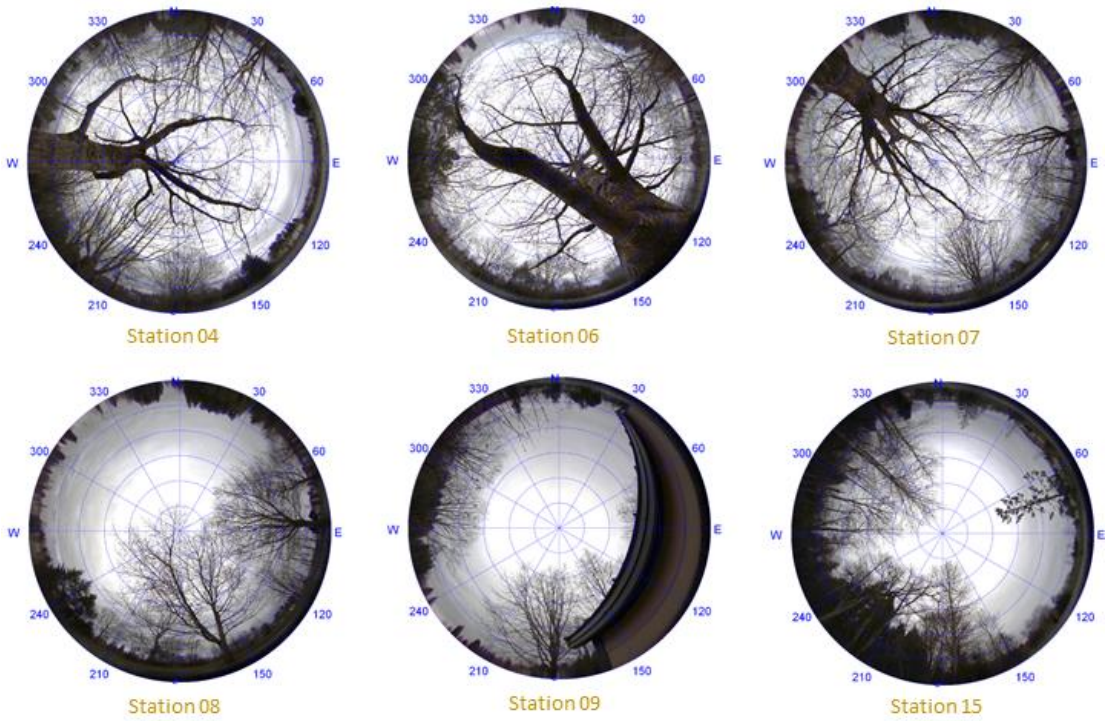


Figure 5. Hemispherical visibility plots of stations with moderate obstructions. The circles shown are 15° vertical angle increments from the top of the fixed height tripod on each station.

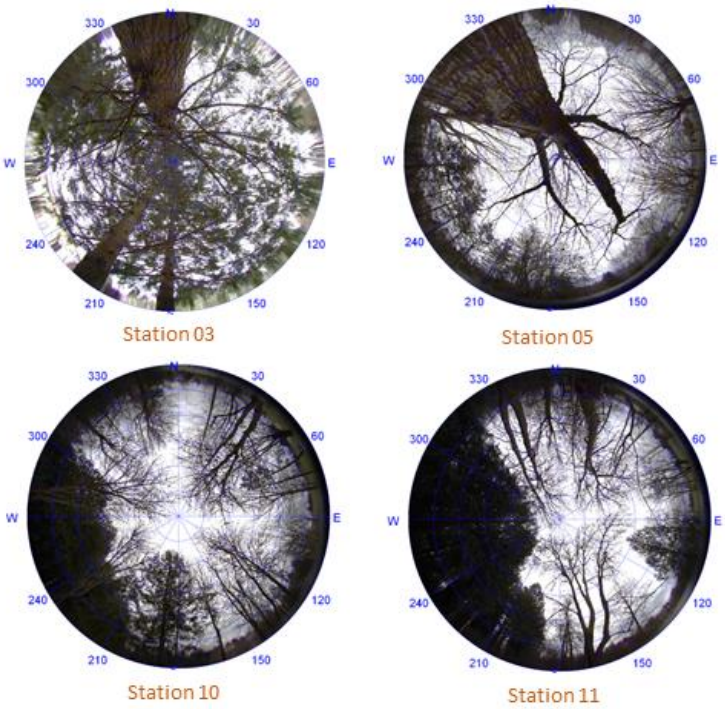


Figure 6. Hemispherical visibility plots of stations with high obstructions. The circles shown are 15° vertical angle increments from the top of the fixed height tripod on each station.

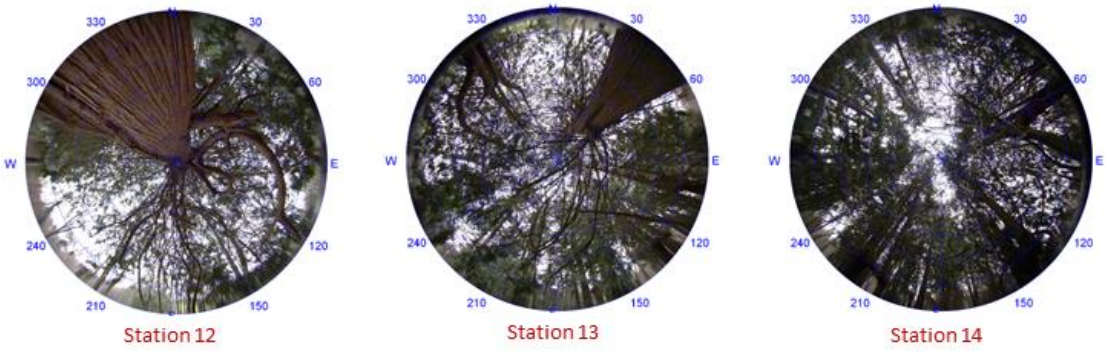


Figure 7. Hemispherical visibility plots of stations with severe obstructions. The circles shown are 15° vertical angle increments from the top of the fixed height tripod on each station.

## 4. Finding Ground Truth

### *4.1 Total Station Survey*

Total station surveys using a Leica TS15p 1” instrument and Leica 360° GRZ122 prism target were performed to provide local precision and accuracy. The instruments were adjusted by a Leica Geosystems certified service center and checked by the author prior to survey. For efficiency, a Leica CS15 controller was used to remotely control the total station. Each station was observed from at least three independent total station setups, with the goal of observing each station from five setups. At one setup per total station survey day, direct and reverse measurements were taken to ensure agreement. The total station was set to average three measurements per observation, resulting in an average of six observations (each of these averaged from 3 measurements) on each station, ranging from 3 to 11 different observations per station.

### *4.2 Static GNSS Survey*

The static GNSS survey consisted of three sessions of an average of 4-hours per session on five stations (Stations 1, 2, 8, 15, 17) in the study site. These stations were selected to balance overhead visibility of the stations with the overall network geometry. Static GNSS observations were collected using five Leica GS14 combined antenna/receivers mounted on 2-m fixed height tripods (Figure 8). The fixed-height tripod level bubbles were checked for calibration prior to use. The field crews targeted three, 5-hour sessions; however, in these three sessions the average overlapping observation duration was approximately 4.4 hours (3.5, 5, and 4.75 hours) due to battery life and other issues. GPS, GLONASS, and Galileo observations were all logged within the static data.

Figure 8. Example photograph of a static GNSS setup with the equipment used in this study (Note this photograph was acquired at different field site)

Static GNSS observations were submitted to both *OPUS-static* and *Trimble CenterPoint RTX Post-Processing Service* (*TrimbleRTX*). Both are web-based static GNSS post-processing tools that require minimal user input and have been shown to perform similarly at observation durations greater than 2 hours (Jamieson and Gillins 2018). These post-processing tools were selected amongst other options because of their differences in processing techniques, available GNSS constellations, and built-in coordinate systems. *OPUS-static* applies relative positioning to GPS-only observations greater than 2 hours in duration; whereas, *TrimbleRTX* applies Precise Point Positioning to GPS, GLONASS, Galileo, BeiDou, and QZSS observations with no minimum duration (but suggested observations greater than 1 hour). Both services can provide coordinates in NAD83(2011) epoch 2010.0; unfortunately however, *TrimbleRTX* implements a global tectonic model and does not fully capture local tectonic plate motion, so the resulting coordinates were corrected to account for plate motion using the National Geodetic Survey (NGS) Horizontal Time-Dependent

Positioning tool, *HTDP*. This correction is on the order of 0.09 m horizontally and 0.01 m vertically.

For an initial investigation of coordinate quality, the solution details were examined and the coordinates provided by *OPUS-static* and *TrimbleRTX* were compared. Notably, one observation from Station 1 triggered an error code and would not process in *OPUS-static*. Five of the 14 *OPUS-static* solutions used less than 50% of observations, all from Stations 8 and 15. Six solutions had less than 80% fixed integer ambiguities (3 from Station 8, 2 from Station 15, and 1 from station 17). *TrimbleRTX* reported standard deviations greater than the 0.015 m threshold for the 2D horizontal component of 7 solutions (3 solutions each from Stations 8 and 15, and 1 solution from Station 02). All *OPUS-static* and *TrimbleRTX* solutions (*HTDP* corrected) agree within a maximum of 0.05 m horizontally and 0.05 m vertically. (The average difference was 0.02 m horizontally and 0.01 m vertically.)

The base station used for the RTK survey consists of a permanent fixture operated by Discovery Management Group. An independent static GNSS survey performed during the establishment of this base station included three stations (Stations 1, 16, 18) in the study site. Static GNSS observations at these stations and the base were adjusted in *OPUS-projects* to determine the final base position with reported coordinate uncertainties of 0.001 m horizontally and 0.003 to 0.004 m vertically (relative to ellipsoid height).

### *4.3 Adjustment*

A least squares adjustment was performed using *MicroSurvey StarNet* with the static GNSS coordinates, static GNSS baselines, and total station observations. Static GNSS coordinates were initially weighted with the uncertainties stated in their respective *OPUS-static*, *TrimbleRTX*, and *OPUS-projects* baseline solutions. Note that in the final adjustment, GNSS coordinate weights were scaled further, as discussed below, to account for overly optimistic estimates of accuracy (Kashani et

al. 2004; Weaver et al. 2018). Static GNSS baselines were weighted with their covariance matrices. The instrument uncertainties were initially set according to manufacturer specifications. Other uncertainties for each component were adjusted slightly to bring the error factors close to unity (1.0) to satisfy the chi-squared test at 95% confidence after removal of outliers. An "error factor" near unity signifies that the residuals of input data approximately equal the formally propagated errors from the stochastic model.

In the final adjustment, the *OPUS-static*, *TrimbleRTX* and *OPUS-projects* coordinate uncertainties were scaled by 5 to improve consistency between them and the network, bringing the coordinate error factor to 0.935. Recall that approximately half of both *OPUS-static* and *TrimbleRTX* solutions had quality indicators indicating poor solution quality; hence, these quality indicators estimated by OPUS and Trimble were not necessarily fully represented by their estimated uncertainties. The *OPUS-projects* solutions had extremely small (and unrealistic) estimated standard deviations (few mm) that needed to be scaled up to fit with the repeated total station measurements. Despite this scaling, the overall uncertainties of the *OPUS-projects* were still smaller than the *OPUS-static* and *TrimbleRTX* uncertainties. This strategy purposely assigns greater weight to the *OPUS-projects* solutions because the rover RTK positions are all directly linked to the RTK base position. Our reasoning for this strategy was to avoid introducing a bias by shifting global coordinates based on other sources. However, the *OPUS-static* and *TrimbleRTX* coordinates helped confirm the validity of the *OPUS-projects* coordinates given that those were completed a year prior to the study survey.

Table 2 summarizes estimated instrument errors as used in the adjustment. Total station observation uncertainties were set using manufacturer specifications and centering errors were adjusted to account for user-introduced uncertainties. The total station angles, distances, and elevation differences had error factors of 0.913, 1.082, and 1.032 respectively. Raw static GNSS baselines were imported and weighted with

their covariance matrices. The computed GNSS baseline uncertainties were scaled by 40 (Kashani et al. 2004) and given a centering error of 0.0005 to achieve an error factor of 0.986. The overall error factor of the adjustment is 0.991, which is centered within the chi-squared test lower and upper bounds of 0.947 and 1.053 at 95% confidence. This indicates that the adjustment is a valid adjustment when compared against the stochastic model.

Table 2. Estimated instrument errors used in least squares adjustment

| System | Parameter | Value |
|---|---|---|
| Total station | Distance* | 0.0020 m + 0.002 ppm |
| | Elevation difference* | 0.0020 m + 0.002 ppm |
| | Angle* | 1 second |
| | Target horizontal and vertical centering error | 0.0019 m |
| GNSS | GPS error scaling factor | 40.0 |
| | GPS centering error | 0.0005 m |

*denotes values are based on manufacturer specifications.

Outliers were considered as a measurement with a ratio of the observation residual to the propagated error estimate greater than 3.0, similar to a 3-sigma test. The adjustment revealed a relatively low number of outliers given the amount of input data. Of the 117 total station observations, only 7 were removed as outliers. Of the 216 GNSS baselines, only 4 were removed as outliers. Of the 32 sets of coordinates, none were removed as outliers.

At 95% confidence, the final adjusted coordinates have estimated horizontal uncertainties ranging from 0.007 m to 0.011 m and vertical uncertainties (relative to ellipsoid height) ranging from 0.019 to 0.021 m. True global uncertainties would be expected to be larger and would propagate from the initial static GNSS coordinate uncertainties.

## 5. RTK GNSS Survey

### *5.1 Field Work*

The RTK survey was completed during a one week period in January 2019. All RTK measurements were referenced to a triple frequency base station consisting of an EOS Arrow Gold receiver and Hemisphere A45 antenna. The base station was located approximately 5.7 km from the project site. Two custom pole setups were utilized as rovers. Each setup had two EOS Arrow Gold receivers connected to one Hemisphere A45 antenna via cable splitter, mounted on a 2-m fixed-height pole with bipod legs. Each receiver connects using the *EOS Tools Pro* app via Bluetooth to an Android device and data logging is controlled by *GNSS Logger* app.

Each receiver was set to a different constellation combination to evaluate four scenarios likely to be used. The configurations are as follows: (1) GPS-only, (2) GPS+GLO, (3) GPS+GAL+BDS, and (4) GPS+GLO+GAL+BDS. For simplicity, throughout the remainder of this paper, we will refer to these scenarios by the number of constellations used in that survey. Notably, other combinations could be used to achieve the same total number of constellations for configurations (1) to (3), but these were selected based on common configurations used for GNSS surveys in North America. Configurations (1) and (2) were chosen because many previous studies assess the impact of GLONASS in addition to GPS satellites. Hence, these provide a baseline of the common approaches used today in North America by most surveyors. Configuration (3) was specifically chosen to utilize only CDMA systems and assess the impact of that difference in signal structure. Configuration (4) uses all four available GNSS constellations that are available to capture the upper bound of using all of the systems.

Throughout the five RTK survey days, the number of satellites used by the (4) constellation configuration ranged from 19 to 33 across the occupations observed. The number of satellites used by the (4) constellation receiver on January 3, 2019 is

indicative of typical conditions throughout the survey (Figure 9). For reference, the total number of theoretically available satellites during the RTK survey from the four constellations ranged from 22 to 34, with a minimum of 7 available GPS satellites. Given that the data are plotted hourly, the apparently abrupt decrease in available satellites shown in the middle of the day actually resulted from a slow decrease in available satellites and coincided with a midday break in the field work.

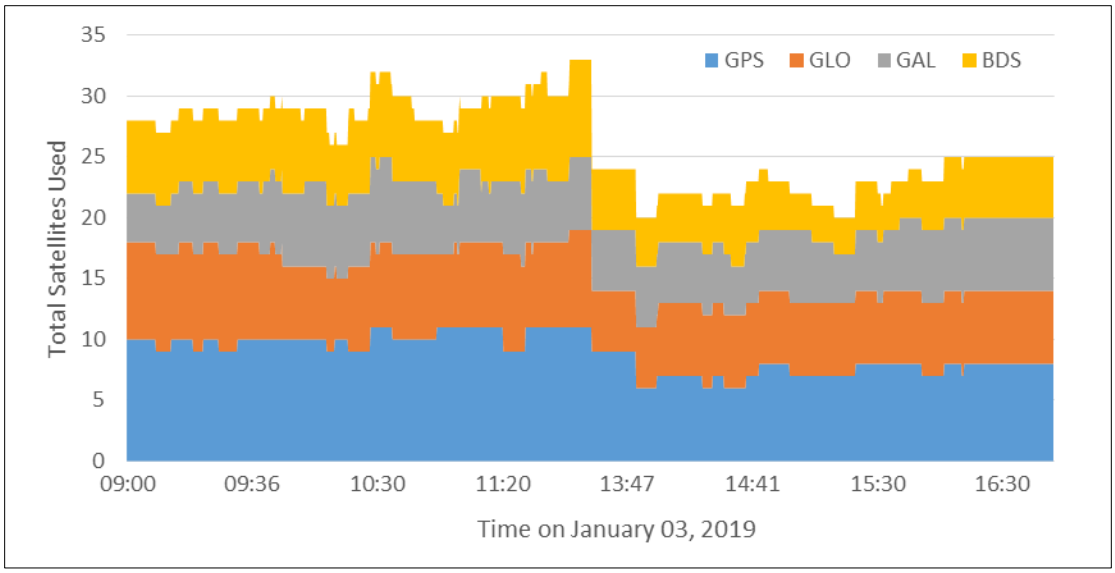


Figure 9. Example of satellite availability during RTK survey, shown in local time on January 03, 2019.

One RTK setup collected configurations (1) and (3) simultaneously. The other RTK setup collected configurations (2) and (4) simultaneously. Two people operated these setups so that one setup of configurations could be observed immediately after the other. The occupations for each of the 4 combinations occurred close together and had very similar satellite conditions. Across 5 days in January 2019, over 100,000 epochs of RTK GNSS data were collected, resulting in approximately 14 occupations per station per setup in the survey. Each station was occupied for 30 seconds if the solution was “fix” and 180 seconds (3 minutes) if solution was “float” upon arrival at the station. A longer occupation time was used for float solutions to provide opportunity for the receiver to achieve a fixed solution as well as maintain a

consistent time to wait for a fixed solution. A similar strategy is common amongst surveyors.

### *5.2 Equipment Testing*

To determine if there were any equipment- and operator-based bias, in a preliminary survey prior to the main RTK survey campaign, we set all of the receivers to observe 4 constellations and occupied each station twice for 30s with each RTK setup. Each of these coordinates was differenced from the reference coordinates, and then we computed the minimum, maximum, range, mean, and standard deviation of these residuals for each receiver. We computed these statistics for stations grouped by obstruction category and for all stations combined.

Statistics for the 2D residuals at grouped low to high obstruction stations are representative of the general trends seen for 2D and 3D residuals. Severely obstructed stations were excluded from the statistics reported here because those stations are prone to extreme outliers and are not representative of comparative equipment performance. Low, moderate, and high obstruction stations were all included to provide a sufficient number of observations to compare.

For low to high obstruction stations, three of the four receivers had mean horizontal residuals between 0.034 and 0.040 m and standard deviations between 0.082 and 0.103 m. The fourth receiver, however, had a mean horizontal residual of 0.065 m and standard deviation of 0.135 m. This receiver consistently used a lower number of BeiDou satellites than other receivers during this test. As a result, it was purposefully chosen to be used for combination (1) GPS-only and appeared to operate as expected under GPS-only conditions.

Overall, based on this analysis, we found no reason to believe the different antennas, receivers, android devices, and equipment operators have any impact on the final coordinates.

### *5.3 Outlier Removal*

In order to most clearly represent the differences between constellations, we did not rigorously remove outliers. The rationale for this decision is that without the numerous repeat occupations we performed in this extensive survey, the typical user performing an ordinary survey would have no way of knowing an occupation may be erroneous based on the information provided in the field to the operator. Only outliers with problems visible to or easily deduced by a typical user, such as those that were likely the result of misnamed stations, were removed.

To remove misnamed stations, we disregarded fixed epochs with horizontal residuals greater than 4 meters. Stations 12 through 14 are each about 5 meters apart. Four meters was chosen given the high and severe obstruction conditions at those stations, likely resulting in larger positioning errors. Epochs with receiver-estimated horizontal uncertainties greater than 0.15 m were disregarded. Finally, any observations with less than 5 satellites used were disregarded, as a proper RTK solution requires a minimum of 5 satellites. In total, these analyses resulted in 1.7% of fixed epochs collected (776 of 46,567) being considered outliers. All of the removed epochs were labeled as observations collected on Stations 10 through 14, all of which were high and severe obstruction stations.

## 6. Results and Discussion

In order to evaluate the impacts of multi-constellation RTK GNSS, we computed the percent of fixed observations, coordinate residuals, RMS values, standard deviations, and bias. Other analyses quantify the relationship between positional accuracy and receiver-estimated precision. Unless otherwise noted, all statistics and plots are based

on residuals for each single epoch (1-second) observed, where each occupation consisted of 30-seconds (epochs) or more in observation length.

### *6.1 Survey Productivity*

To assess productivity impacts from the additional constellations, the percent of fixed observations for each constellation scenario were computed for each station as well as for each obstruction category. The percent of fixed solutions is a good indicator of conditions encountered in the field when performing RTK surveys as a fixed, not float, solution is a standard practice in engineering surveying work. Table 3 shows the percent of fixed epochs by obstruction category for each constellation combination. The percent of fixed epochs by station are available in the Appendix. Figure 10 shows the percent of fixed epochs versus obstruction category for each constellation combination. Note that these values represent the number of fixed epochs and not the number of fixed occupations, since observations were 180s for float solutions and 30s for fix solutions. Despite this discrepancy, useful trends are still shown.

At low obstruction stations, the percent of fixed epochs is similar for all constellation scenarios. However, as obstructions increase, there is a clear benefit to additional constellations to obtain fixed solutions. At high obstruction stations, (2) GPS+GLO had 20.9% fixed epochs while (3) and (4) constellations had over 70% fixed epochs. At severe obstruction stations, (2) GPS+GLO and (1) GPS-only each achieved one fixed observation with 0.6% and 2.4% fixed epochs, respectively; In contrast, (3) and (4) constellations performed similar to one another with 21.5% and 24.4% fixed epochs, respectively. Moving forward, it is important to keep in mind these limited sample sizes, particularly relative to the number of occupations.

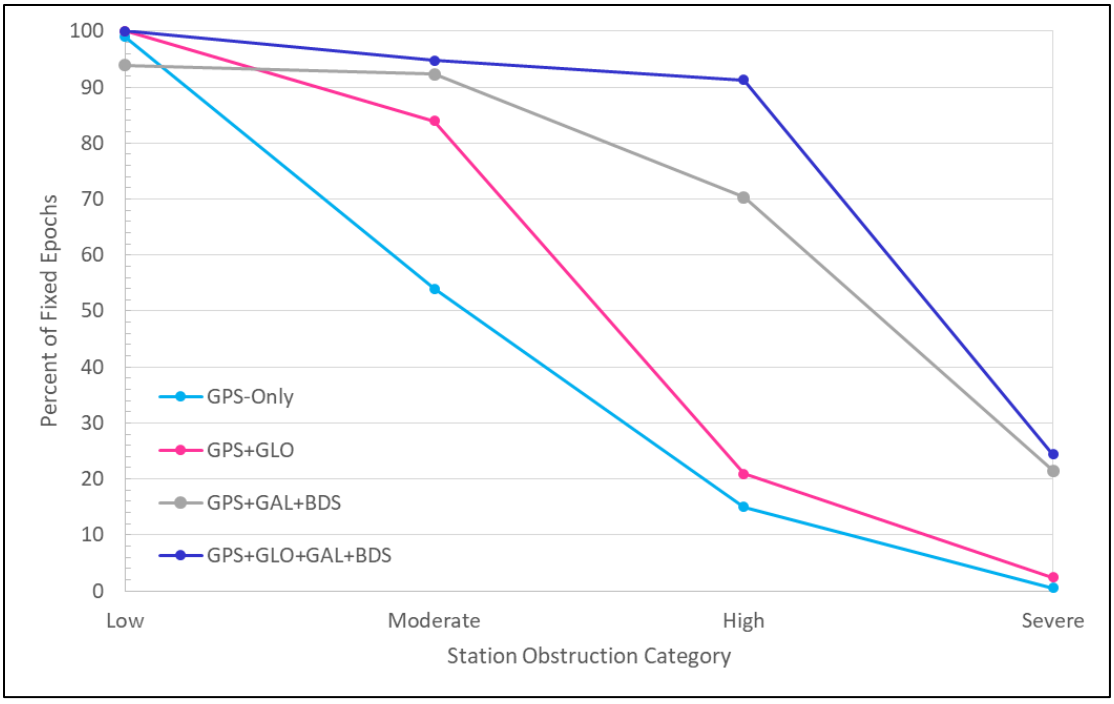


Figure 10. Percent of fixed epochs versus obstruction category for each constellation combination.

Table 3. Number of total and fixed epochs for each obstruction category and constellation combination.

| | GPS-ONLY | | | GPS+GLO | | | GPS+GAL+BDS | | | GPS+GLO+GAL+BDS | | |
|---|---|---|---|---|---|---|---|---|---|---|---|---|
| Obstruction | n (total) | n (fixed) | % fixed | n (total) | n (fixed) | % fixed | n (total) | n (fixed) | % fixed | n (total) | n (fixed) | % fixed |
| Low | 3257 | 3223 | 99.0 | 3246 | 3246 | 100.0 | 2917 | 2738 | 93.9 | 4297 | 4297 | 100.0 |
| Moderate | 4787 | 2583 | 54.0 | 3353 | 2815 | 84.0 | 3841 | 3545 | 92.3 | 4573 | 4335 | 94.8 |
| High | 8065 | 1206 | 15.0 | 7786 | 1628 | 20.9 | 6343 | 4462 | 70.3 | 8009 | 7309 | 91.3 |
| Severe | 5575 | 32 | 0.6 | 7724 | 188 | 2.4 | 6279 | 1351 | 21.5 | 11598 | 2833 | 24.4 |

The raw percent of fixed epochs alone is not entirely indicative of productivity because an erroneous fixed solution would not be useful; the occupation would need to be repeated, resulting in a far less productive survey. A thorough discussion of coordinate accuracy is provided in the next section; however, for the context of productivity, Figure 11 shows the percent of fixed solutions with horizontal and vertical residuals less than 0.15, 0.10, and 0.05 m. While Figure 10 shows the

productivity a typical user would experience in the field, Figure 11 represents a more realistic quantification of productivity of the survey.

In contrast to Figure 10, Figure 11 shows that (3) and (4) constellations are not always the most productive. The user may be more likely to obtain a fixed solution with the additional satellites as shown in Figure 10; however, that solution is not necessarily more likely to be within acceptable accuracy ranges as shown in Figure 11. Although all constellation combinations perform similarly at low and moderate obstruction both horizontally and vertically, at high and severe obstruction levels (4) constellations is most productive for horizontal positioning. At high obstruction, (2) and (3) constellations perform similarly in the horizontal direction, with GPS-only being significantly less productive. In the vertical direction, the constellation combinations generally perform similarly for all obstruction categories. Notably, however, GPS+GLO (2) is somewhat more productive at high obstruction stations, and (3) and (4) constellations are somewhat more productive at severe obstruction stations.

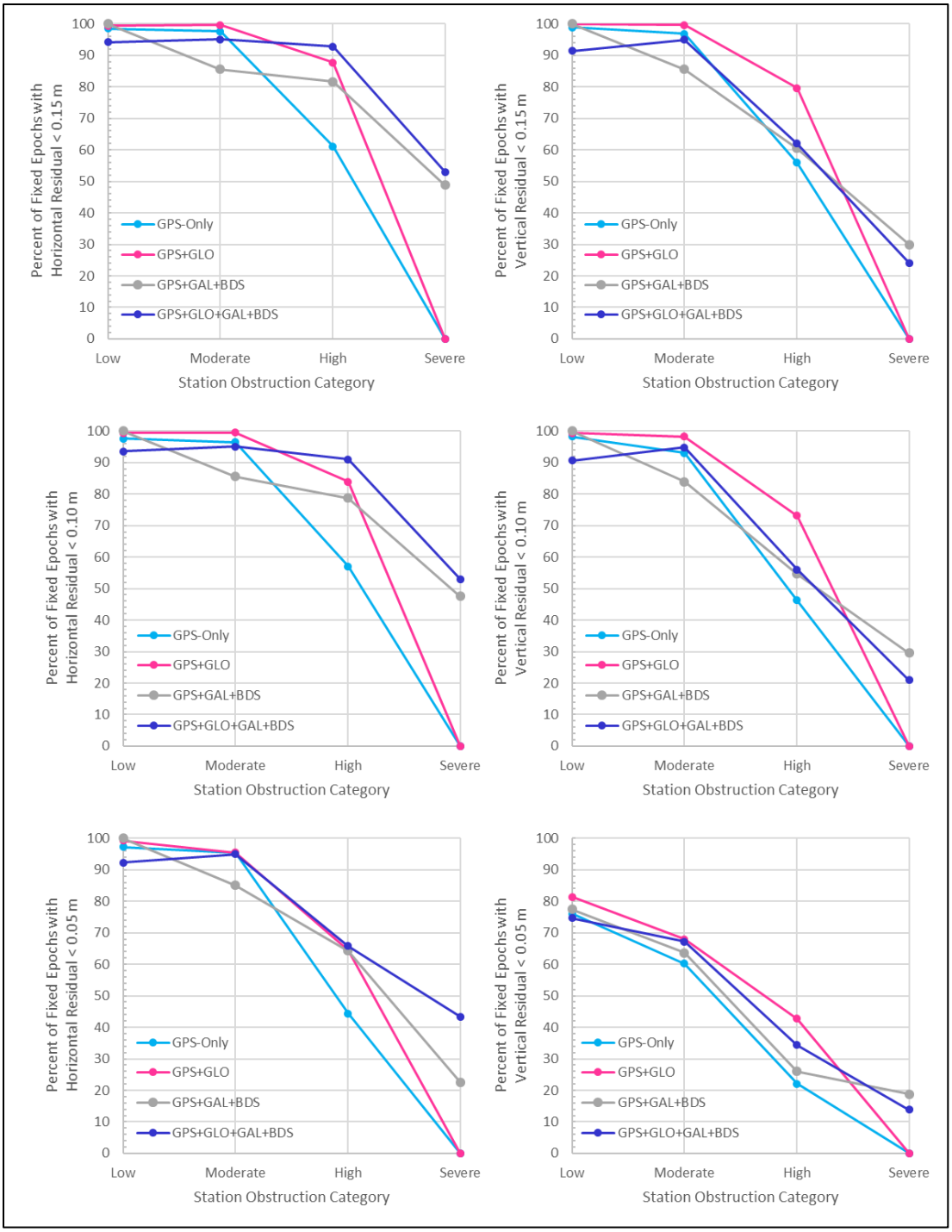


Figure 11. Percent of fixed epochs with horizontal and vertical residual less than 0.15, 0.10, and 0.05 meters.

### *6.2 Coordinate Accuracy*

To evaluate coordinate accuracy, we differenced each fixed epoch of the RTK survey coordinates from the final adjusted coordinates in the easting, northing, and up directions. We analyzed residuals and RMS values in each direction, as well as a combined 2D horizontal direction. Note that vertical residuals and RMS values are in terms of ellipsoid height. Unless otherwise noted, all plots in this section use only fixed epochs that are not classified as outliers as per the previous section.

First, we evaluated the horizontal residual of fixed solutions versus the number of satellites, regardless of the specific constellation those satellites are in (Figure 12). For low to high obstruction categories, there is no observable trend between the horizontal residual and number of satellites. For severe obstruction stations, additional satellites show a slight trend of reducing the horizontal residual, albeit with a low fit quality ($y = -0.06x+1.5$, $R^2 = 0.05$). Another plot for horizontal residuals versus number of GPS satellites showed no clear trend for any of the obstruction categories.

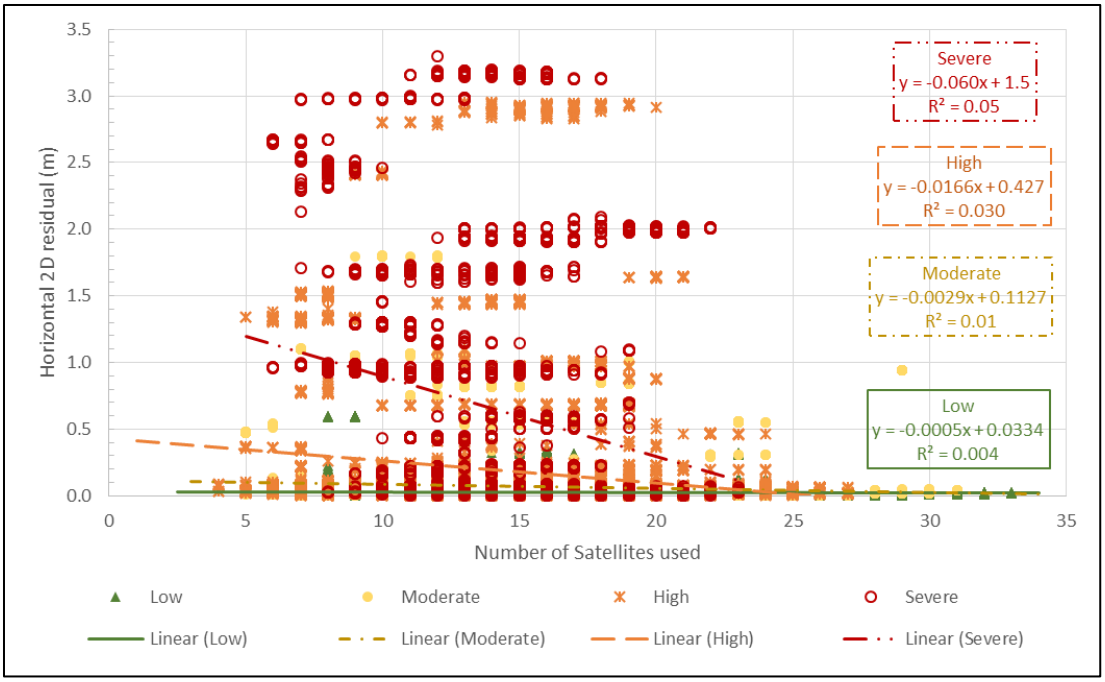


Figure 12. Horizontal residual versus total number of satellites used, regardless of constellation.

Figure 13 provides the horizontal and vertical RMS values versus obstruction category. A more detailed table with specific values is provided in the Appendix. RMS values by station are also available in the Appendix. Note again the limited sample sizes at high and severe obstruction, particularly for the GPS and GPS+GLO combinations (Table 3). At low and moderate obstruction, all constellations generally perform similarly horizontally. At low obstruction, (4) constellations show a larger vertical RMS values than other constellation combinations. At high and severe obstruction levels, additional constellations generally reduce horizontal and vertical RMS values. GPS+GLO shows exceptionally small horizontal and vertical RMS values at high obstruction. The small (2) GPS+GLO RMS values at high obstruction could be relative outliers due to the small number of fixed epochs. The larger RMS values for (3) and (4) constellations may be explained by inter-system biases or potentially poor combination of observables in the receiver software. Unfortunately, since corrections occur in real time, the data cannot be reprocessed using a receiver software update with improved algorithms without repeating the field work.

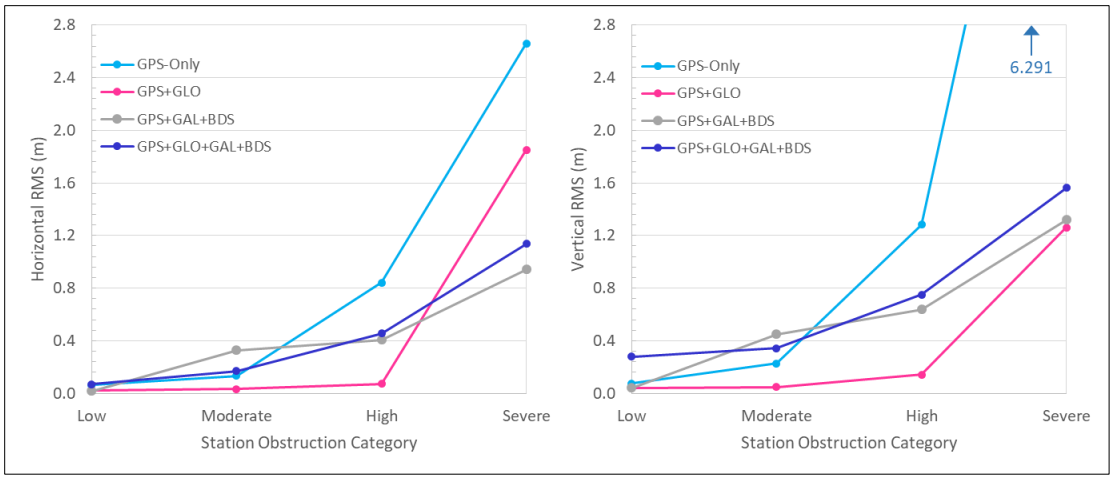


Figure 13. Horizontal and vertical RMS values versus station obstruction category, plotted by constellation combination.

Figure 14 shows the horizontal and vertical RMS values versus obstruction category for each individual station, with stations labeled for RMS values greater than 0.5 m. This figure highlights the spread in RMS values for each constellation combination to identify any particularly high or low stations. Note that (1) GPS-only and (2) GPS+GLO did not achieve any fixed solutions on two of three severe obstruction stations. GPS+GLO generally has the lowest spread in horizontal and vertical RMS values; the exception being horizontal RMS values at Station 13, where GPS+GLO achieved only two fixed occupations with 188 seconds of data. Nevertheless, when GPS+GLO achieves a fixed solution, the resulting RMS values tend to be very small.

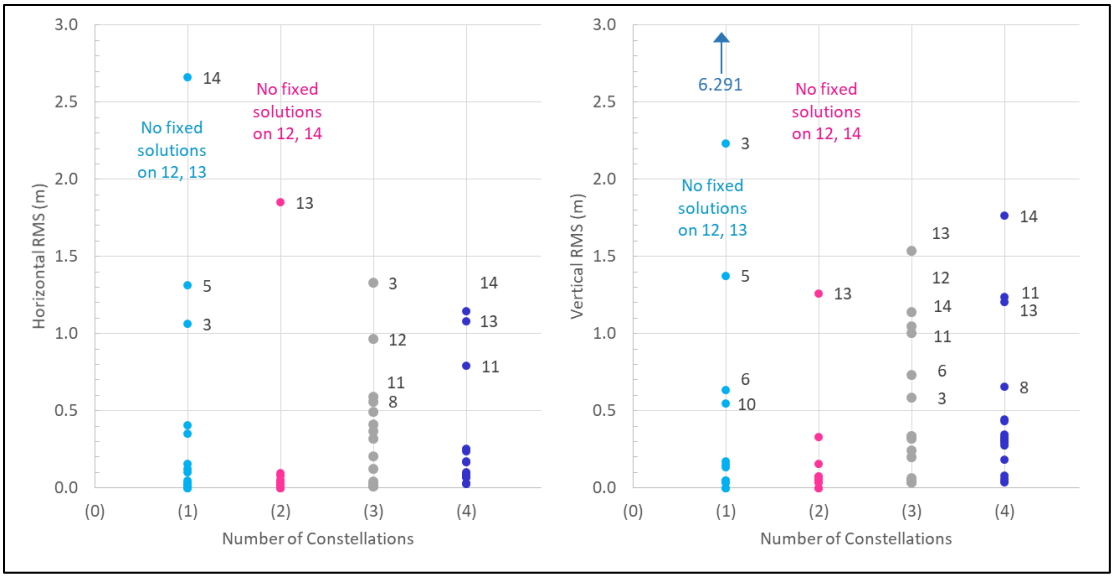


Figure 14. Station horizontal and vertical RMS values versus number of constellations, labels indicate stations with RMS values greater than 0.5 m.

RMS considers both bias, or systematic error, and precision. Precision is quantified with the standard deviation of the residuals (Figure 15 and Table 4). The standard deviation generally increases with obstruction category and GPS+GLONASS (2) shows lower standard deviations than other configurations. Amazingly, one GPS-only occupation achieved 32 seconds of fixed solutions during one occupation of severe obstruction stations with a horizontal and vertical standard deviation of 0.008 m and 0.026 m, respectively (Table A4). This low standard deviation is excluded from Figure 15 given that it is only one occupation and likely not repeatable. This standard deviation is typical for the variation in epochs within one occupation, for any obstruction category or constellation combination. In other words, the variation in coordinates occurs between occupations not between epochs.

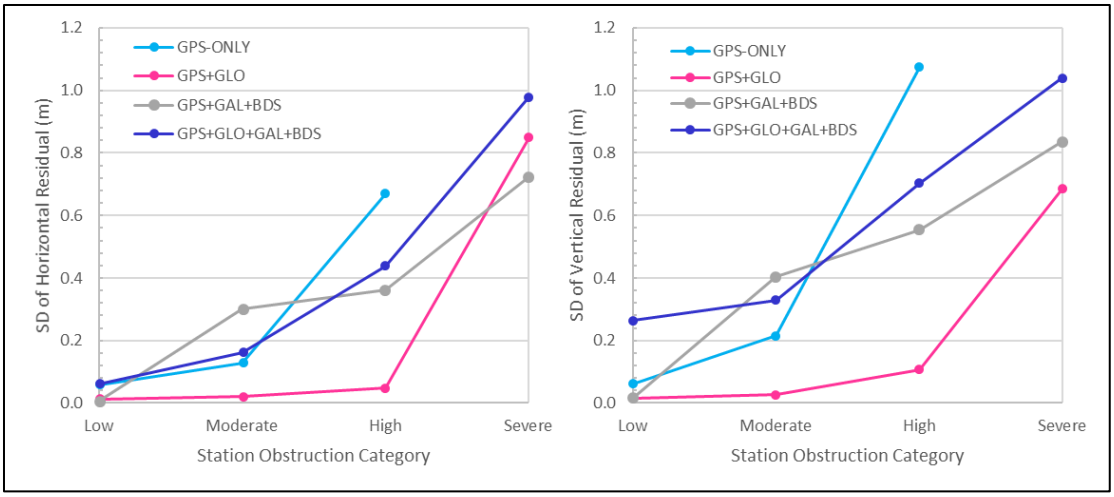


Figure 15. Standard deviation of horizontal and vertical residual versus obstruction category for each constellation.

Bias was computed as the arithmetic mean of the residuals in each direction. Figure 16 and Table 4 show the horizontal and vertical bias for each constellation combination per obstruction category. Biases computed individually for the easting and northing directions is included in the Appendix. At low and moderate obstruction stations, the bias is consistently close to zero for all constellation combinations. In contrast, at severely obstructed stations, all constellation combinations show some bias, with bias being most prominent with (1) GPS-only and (2) GPS+GLO. In cases of detected bias, most of the bias would be expected to reside in the RTK coordinates rather than the reference network given that the reference coordinates were derived using a total station, which provided high relative accuracy. Lastly, when interpreting these results it is important to remember the small sample sizes for GPS-only and GPS+GLO at severe obstruction.

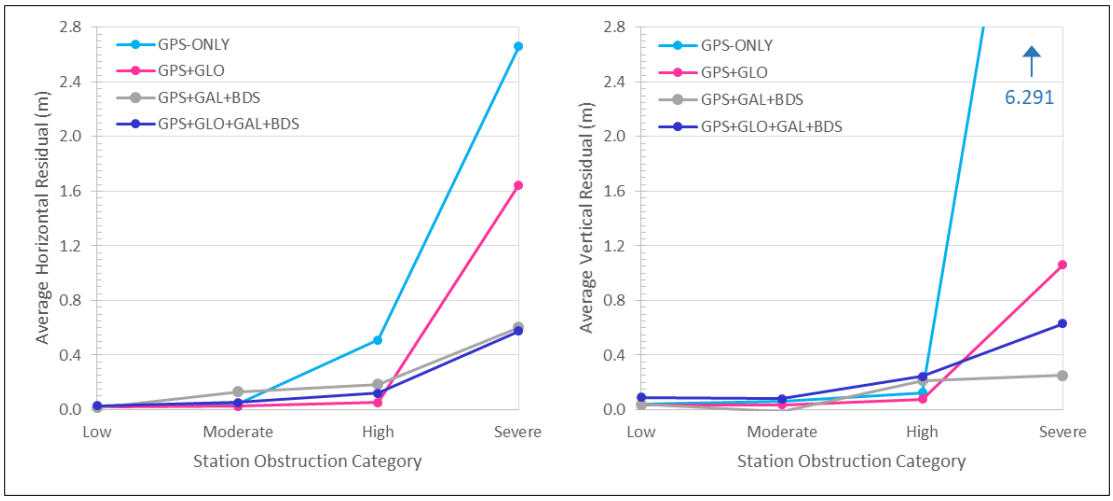


Figure 16. Average horizontal and vertical residual versus obstruction category for each constellation combination.

Table 4. Standard deviation and average residual in meters in horizontal and vertical directions for each obstruction category and constellation combination.

| | GPS-ONLY | | GPS+GLO | | GPS+GAL+BDS | | GPS+GLO+GAL+BDS | |
|---|---|---|---|---|---|---|---|---|
| **Obstruction** | **mean ΔH (m)** | **SD ΔH (m)** | **mean ΔH (m)** | **SD ΔH (m)** | **mean ΔH (m)** | **SD ΔH (m)** | **mean ΔH (m)** | **SD ΔH (m)** |
| Low | 0.024 | 0.059 | 0.018 | 0.013 | 0.015 | 0.005 | 0.037 | 0.073 |
| Moderate | 0.039 | 0.128 | 0.024 | 0.020 | 0.131 | 0.301 | 0.052 | 0.156 |
| High | 0.513 | 0.669 | 0.054 | 0.048 | 0.185 | 0.361 | 0.119 | 0.428 |
| Severe | 2.662 | 0.008 | 1.647 | 0.849 | 0.603 | 0.723 | 0.549 | 0.934 |
| **Obstruction** | **mean ΔUp (m)** | **SD ΔUp (m)** | **mean ΔUp (m)** | **SD ΔUp (m)** | **mean ΔUp (m)** | **SD ΔUp (m)** | **mean ΔUp (m)** | **SD ΔUp (m)** |
| Low | 0.043 | 0.062 | 0.038 | 0.016 | 0.039 | 0.016 | 0.121 | 0.296 |
| Moderate | 0.071 | 0.215 | 0.040 | 0.027 | 0.196 | 0.403 | 0.095 | 0.328 |
| High | 0.702 | 1.074 | 0.094 | 0.108 | 0.316 | 0.555 | 0.251 | 0.685 |
| Severe | 6.291 | 0.026 | 1.060 | 0.686 | 1.021 | 0.836 | 1.094 | 1.019 |

Figure 17 and Figure 18 plot the horizontal and vertical residual versus station number, grouped by constellation combination. These figures additionally illustrate the bias (as average residual) and standard deviation given in Table 4 and Figure 16. Average horizontal and vertical residual versus obstruction category for each constellation combination. For example, (1) GPS-only showed a bias on severe obstructed stations in all directions. GPS-only had one fixed solution occupation on severe obstruction stations at Station 14. The residuals for the epochs in this single occupation are greater than 2.5 m horizontally and 6 m vertically. The 32 epochs

agree very closely as the points appear overlapping. Thus, this occupation is showing a small standard deviation and large average residual.

Figure 17 and Figure 18 also reveal useful information about the high RMS values occurring at low-obstruction stations from four constellations. It seems there are a few occupations that have a bias as high as 0.3 m horizontally and 1.3 m vertically. These occupations predominantly occur within one round of data collection, meaning they occurred one after the other at successive stations. This one erroneous round could be the cause of the relatively large vertical RMS values at low obstruction stations seen earlier in Figure 13.

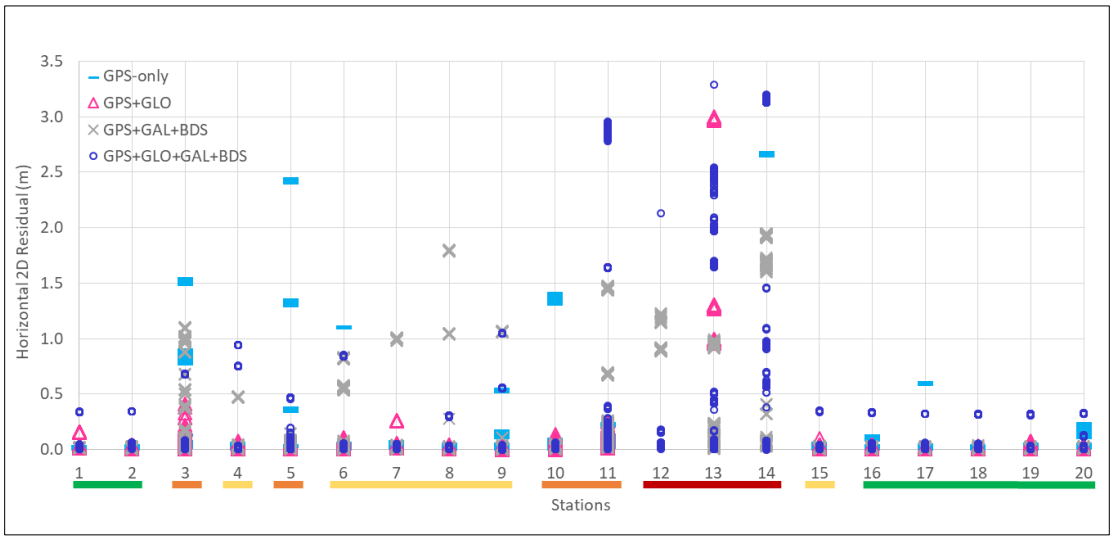


Figure 17. Horizontal residual versus station, grouped by constellation combination.

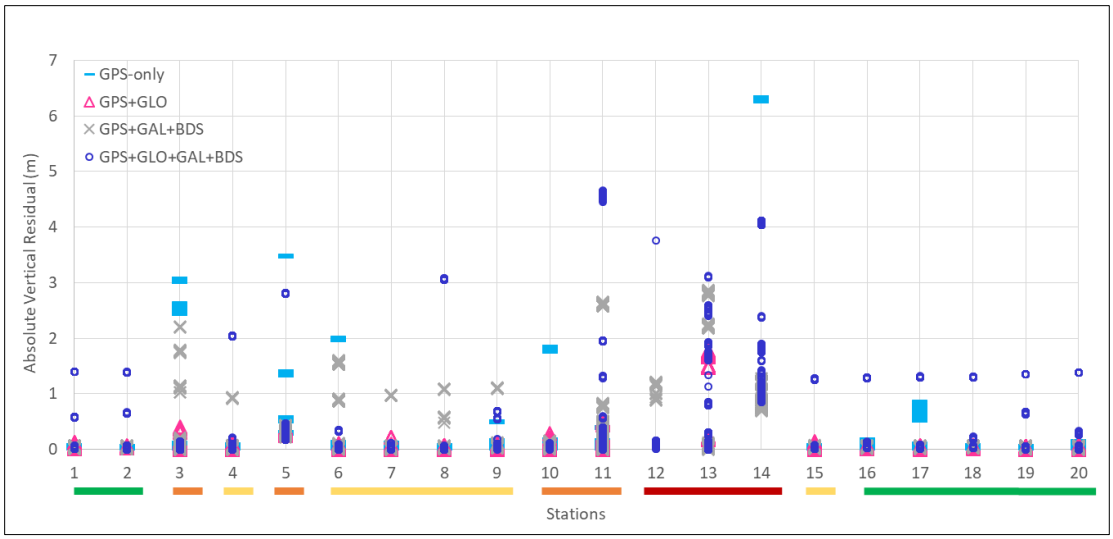


Figure 18. Vertical residual versus station, grouped by constellation combination.

### *6.3 Receiver-estimated precision*

As the user collects data, the receiver estimates and reports coordinate precision in real-time. Ideally, this estimated precision would be related to the overall coordinate accuracy, so that the operator can judge the quality of data in the field and repeat/verify observations as necessary. Some receivers, including those used in this RTK survey, call these estimated precisions “RMS”, incorrectly leading many users to believe these values can serve as coordinate accuracy or estimated error. Each receiver manufacturer estimates precision in their own way; subsequently, the results from this study may or may not be indicative of performance using other receiver manufacturers.

Figure 19 plots the horizontal residual versus receiver-estimated horizontal precision for each fixed epoch, for each constellation combination, grouped by obstruction category. The gray dashed line shows a 1:1 relationship, meaning points on this line would have correctly estimated error, and points above the dashed line have a smaller estimated error than the actual error. Note that only the horizontal case is analyzed here simply for clarity; as seen in the earlier accuracy and bias analysis, differences between constellation combinations are more clear in the horizontal direction.

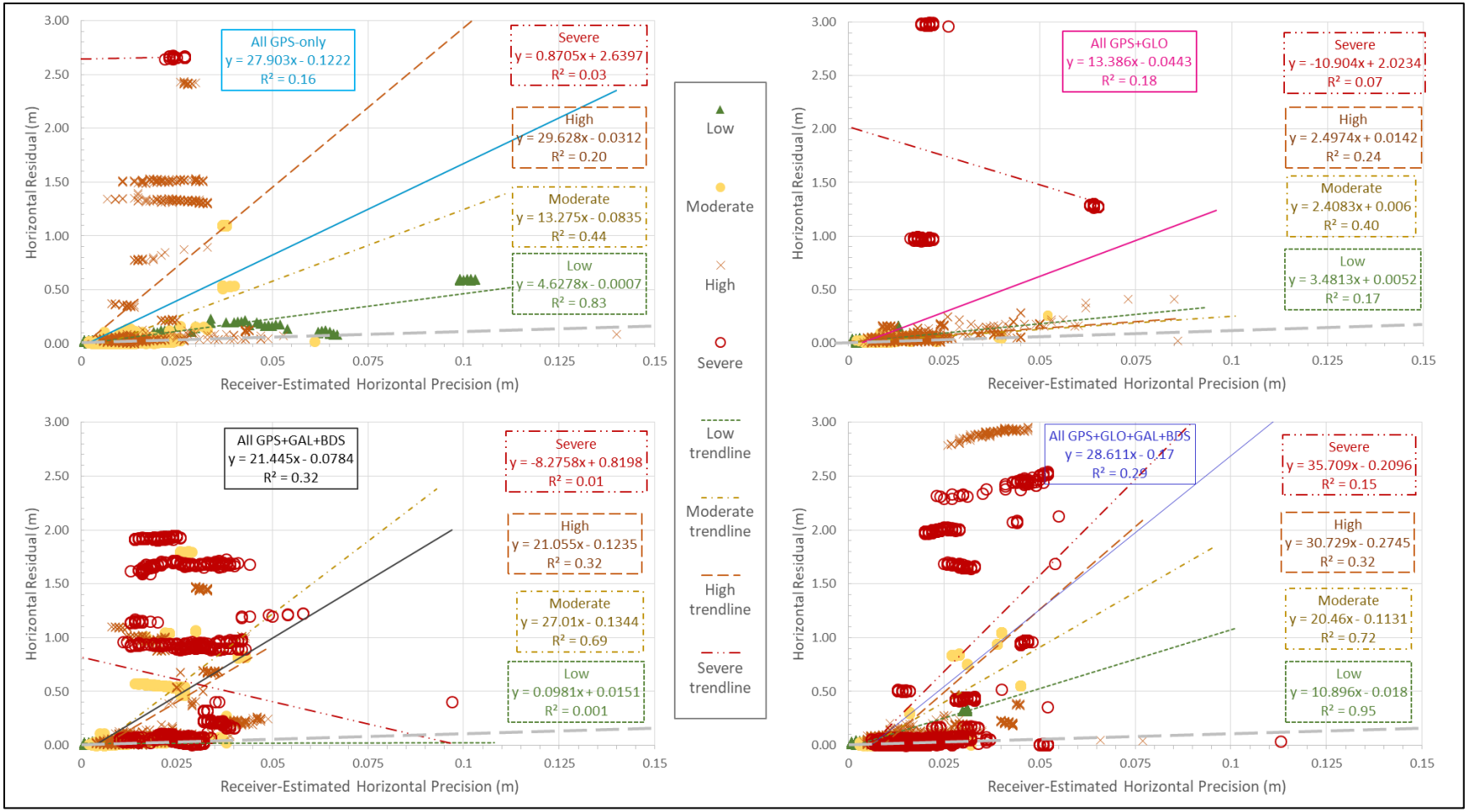


Figure 19. Horizontal residual versus receiver-estimated horizontal precision for each constellation combination, grouped by obstruction category.

Generally, we found the receivers used in this study reported horizontal precision almost 18x lower than the computed horizontal residuals with an $R^2 = 0.19$ (see Appendix). In other words, the receiver was very optimistic and underestimated the error. For observations using GPS-only, the receiver reported horizontal precision values 28x lower than the computed horizontal residuals with $R^2 = 0.16$. For observations using all four constellations, the receiver reported horizontal precision more than 29x lower than the computed horizontal residuals with $R^2 = 0.29$. When grouped by constellation combination, the least optimistic estimated precision (GPS+GLO, $R^2 = 0.18$) was 13x lower than the computed horizontal.

At lower obstruction, the receiver is generally less optimistic compared with higher obstruction levels. For observations using GPS-only under low obstruction conditions, the receiver reported horizontal precision values 5x lower than the computed horizontal residuals with $R^2 = 0.83$. For GPS-only under high obstruction conditions, the receiver reported horizontal precision values 30x lower than the computed horizontal residuals with $R^2 = 0.20$. For observations using all four constellations under low obstruction conditions, the receiver reported horizontal precision values 11x lower than the computed horizontal residuals with $R^2 = 0.95$. For observations using four constellations under high obstruction conditions, the receiver reported horizontal precision values 31x lower than the computed horizontal residuals with $R^2 = 0.32$.

In summary, the slope coefficient of the trendline generally decreases (meaning the receiver is less optimistic) with lower obstruction, though all cases are still highly optimistic. The slope is not clearly impacted by additional constellations. The correlation of the trendline ($R^2$) generally increases with additional constellations and with lower obstruction, meaning the receiver is more consistently estimating precision in these cases but has more trouble estimating precision at higher obstruction levels.

These results may initially appear inconsistent with those documented in Penna et al. (2012), who found estimated coordinate quality to generally correspond to horizontal accuracy. They also found GPS+GLO was slightly more optimistic than GPS-only, where we found GPS+GLO to be the least optimistic of the four constellation combinations. However, we found the estimated precision to generally be more optimistic with additional constellations. The disagreement between results is likely due to use of different receivers as well as the more extreme levels of obstruction conditions in this study compared with much lower levels in Penna et al. (2012). Hence, the findings of Penna et al. (2012) fit within the trends observed in Figure 18, but would be outside the range of obstructions evaluated in this study. Notably, manufacturers have different methods of estimating precision, and it appears the receivers used in this study may be less effective at estimating general coordinate precision.

## 7. Conclusions

In this study, we evaluate survey productivity and coordinate accuracy of single-base RTK GNSS at a test site in North America consisting of 20 stations using different constellations under a variety of forested obstruction conditions, ranging from low to severe. The constellation combinations considered are: (1) GPS-only, (2) GPS+GLO, (3) GPS+GAL+BDS, and (4) GPS+GLO+GAL+BDS. Significant contributions of this study compared to prior work are the consideration of sites with much higher obstruction, predominantly forested obstructions, and located in North America where previous works have been minimal due to limited Galileo and BeiDou satellite availability. Another unique component of this study is the direct comparison of two constellation combinations simultaneously, due to the use of two receivers connected to one antenna; where combinations (1) and (3) were tested simultaneously and combinations (2) and (4) were tested simultaneously.

Reference coordinates for each station in the test site were computed through a rigorous, combined static GNSS and total station survey adjusted by least squares. The static GNSS survey consisted of three 4-hour sessions and the total station survey achieved an average of six independent observations per station. Horizontal and vertical reference coordinate estimated accuracies are less than 0.007 m and 0.011 respectively at 95% confidence. The RTK survey used a single-base located approximately 5.7 km from the study site. Two custom setups each with two receivers connected to one antenna were implemented in order to observe all constellation combinations in close succession.

Additional constellations dramatically improved productivity in the field by achieving a higher percentage of fixed solutions at each station. At low obstruction, only a slight increase was observed since fixed rates were already high with GPS-only. At moderate obstruction, the percent of fixed epochs increased from 54% to 95% from (1) to (4) constellations. At high obstruction, the percent of fixed epochs increases with additional constellations from 15%, 21%, 70%, to 91%. The percent of fixed epochs represents productivity as measured in the field, but ultimately productivity depends on coordinate accuracy. The percent of fixed epochs with horizontal and vertical residuals less than a threshold of 0.10 m generally increases with additional constellations at high and severe obstruction. At high obstruction in the vertical direction, GPS+GLO achieved a greater percent of fixed epochs with residuals less than 0.10 m. In summary, these increases in fixed observations and acceptable fixed observations were observed to be most substantial for higher levels of obstructions; however, severe obstructed stations still had a relatively low fixed epoch rate (24% for 4 constellations with 53% of acceptable fixed solutions at 0.10 m) that would ultimately still result in an unproductive survey using GNSS.

In contrast to the clear results related to productivity, the impact to accuracy of additional constellations is less clear and in some cases the fixed solutions provided by the additional constellations do not result in accurate coordinates, especially when working with severe levels of obstruction. Where GPS+GLO achieved a fixed solution, it generally performed the best across all obstruction categories. At low and moderate obstruction categories, all constellation categories perform similarly, except for (4) constellations that show higher vertical RMS values. (3) and (4) constellations perform similarly at all obstruction conditions, with (4) constellations having slightly larger horizontal and vertical RMS values at high and severe obstruction. At high and severe obstruction marks, GPS-only (1) has significantly larger horizontal and vertical RMS values than other combinations.

Lastly, for all stations and constellation combinations, the receiver-estimated precision was approximately 18x lower than horizontal residual. In other words, the receiver was dramatically optimistic about the actual quality of the coordinates being obtained. The receivers used in this study tended to better estimate precision at low obstruction stations and when using (4) constellations. For observations using GPS-only, the receiver reported horizontal precision 5x ($R^2 = 0.83$) and 30x ($R^2 = 0.20$) lower than the computed horizontal residuals at stations with low obstruction and high obstruction, respectively. For observations using four constellations, the receiver reported horizontal precision 11x ($R^2 = 0.95$) and 31x ($R^2 = 0.32$) lower than the computed horizontal residuals at low obstruction and high obstruction, respectively.

### *7.1 Limitations and Future Work*

Galileo and BeiDou have only recently become practical for global use. As a result, the algorithms utilized within software to combine the observations from the different systems to achieve a solution likely will continue to improve. From this study, it appears that these additional constellations do indeed add some noise to the data that could be reduced. The author would like to see additional data collection to evaluate this change over time. As an example, given that only four constellation scenarios

were evaluated to enable the research team to also evaluate other aspects such as obstruction condition, additional constellation combinations could be analyzed. For example, Galileo and BeiDou were always observed together in this study but these systems could be analyzed separately in future work. While GPS-only is useful for this initial study to provide a baseline, it could be excluded from future work to accommodate other combinations and in the interest of field efficiency.

The data collection for this study was conducted in the western United States, at latitudes near 45° north, with natural (not urban) obstructions. Data collected in other regions may have significantly more or less available satellites due to latitude and the availability of regional systems. Sites in more urban areas may have different results due to differences in multipath between urban canyon and forested environments. Future work could evaluate how the type of obstruction impacts the coordinate quality. A more detailed characterization of overhead conditions could better account for vegetation density in a quantitative way. Similarly, the study could be completed in a leaves-on versus leaves-off comparison to better quantify that impact.

## 8. References

Allahyari, M., Olsen, M. J., Gillins, D. T., and Dennis, M. L. (2018). "Tale of Two RTNs: Rigorous Evaluation of Real-Time Network GNSS Observations." Journal of Surveying Engineering, 144(2), 05018001.

Deng, C., Tang, W., Liu, J., and Shi, C. (2014). "Reliable single-epoch ambiguity resolution for short baselines using combined GPS/BeiDou system." GPS Solutions, 18(3), 375–386.

*EOS Tools Pro* [Android Application]. Eos Positioning Systems Inc. Version 1.49.24.

*GNSS Logger* [Android Application]. Skeele, Ryan, Discovery Management Group Inc. Version 1.0.

*HTDP, Horizontal Time-Dependent Positioning* [Computer Software]. National Oceanic and Atmospheric Administration, National Geodetic Survey, Silver Spring, MD.

Jamieson, M., and Gillins, D. T. (2018). "Comparative Analysis of Online Static GNSS Postprocessing Services." Journal of Surveying Engineering, 144(4), 05018002.

Kashani, I., Wielgosz, P., and Grejner-Brzezinska, D. A. (2004). "On the reliability of the VCV Matrix: A case study based on GAMIT and Bernese GPS Software." GPS Solutions, 8(4), 193–199.

Li, X., Ge, M., Dai, X., Ren, X., Fritsche, M., Wickert, J., and Schuh, H. (2015). "Accuracy and reliability of multi-GNSS real-time precise positioning: GPS, GLONASS, BeiDou, and Galileo." Journal of Geodesy, 89(6), 607–635.

Martin, A., and McGovern, E. (2012). "An Evaluation of the Performance of Network RTK GNSS Services in Ireland." 20.

Msaewe, H. A., Hancock, C. M., Psimoulis, P., Roberts, G. W., Bonenberg, L., and Ligt, H. de. (2017). "Investigating multi-GNSS performance in the UK and China based on a zero-baseline measurement approach." 102, 186–199.

Odolinski, R., and Denys, P. (2015). "On the Multi-GNSS RTK Positioning Performance in New Zealand."

Odolinski, R., Teunissen, P. J. G., and Odijk, D. (2015). "Combined BDS, Galileo, QZSS and GPS single-frequency RTK." GPS Solutions, 19(1), 151–163.

*OPUS-Projects* [Computer Software]. National Oceanic and Atmospheric Administration, National Geodetic Survey, Silver Spring, MD.

*OPUS-Static* [Computer Software]. National Oceanic and Atmospheric Administration, National Geodetic Survey, Silver Spring, MD.

Oregon Department of Transportation. (2018). "About the ORGN." Oregon Real-Time GNSS Network, <https://www.oregon.gov/ODOT/ORGN/Pages/about-us.aspx> (May 16, 2019).

Penna, N., Clarke, P., King, M., and Edwards, S. (2012). Further Testing of Commercial Network RTK GNSS services in Great Britain.

*Skyplotter* [Computer Software]. Javadnejad, F., Gillins, D.T., Jenny, B. “SkyPlotter – Automated GNSS visibility diagrams.”

*Trimble GNSS Planning* [Computer Software]. Trimble, Inc. “GNSS Planning Online,” version 1.4.0.0

Van Sickle, J. (2015). GPS for land surveyors. CRC Press, Taylor & Francis Group, Boca Raton.

Weaver, B., Gillins, D. T., and Dennis, M. (2018). “Hybrid Survey Networks: Combining Real-Time and Static GNSS Observations for Optimizing Height Modernization.” Journal of Surveying Engineering, 144(1), 05017006.

Xi, R., Chen, H., Meng, X., Jiang, W., and Chen, Q. (2018). “Reliable Dynamic Monitoring of Bridges with Integrated GPS and BeiDou.” Journal of Surveying Engineering, 144(4), 04018008.

## 9. Appendix

The appendix includes statistics and figures that were excluded from the general text for brevity but are provided here for completeness. RMS values (Table A1) and fixed epochs (Table A2) are listed by station for each constellation combination. Table A3 lists RMS values by constellation combination, grouped by obstruction category for horizontal, vertical, and 3D directions. Table A4 includes RMS values, standard deviation, and estimated bias by obstruction category for easting, northing, and up directions. Figures A1 and A2 show computed horizontal residual versus receiver-estimated precision, grouped respectively by obstruction category and constellation combination.

Table A1. RMS values by station and constellation combination.

| | GPS-only | | | GPS+GLO | | | GPS+GAL+BDS | | | GPS+GLO+GAL+BDS | | |
|---|---|---|---|---|---|---|---|---|---|---|---|---|
| Station | HRMS (m) | VRMS (m) | 3DRMS (m) | HRMS (m) | VRMS (m) | 3DRMS (m) | HRMS (m) | VRMS (m) | 3DRMS (m) | HRMS (m) | VRMS (m) | 3DRMS (m) |
| 1 | 0.016 | 0.041 | 0.044 | 0.038 | 0.046 | 0.060 | 0.016 | 0.044 | 0.047 | 0.075 | 0.319 | 0.328 |
| 2 | 0.017 | 0.039 | 0.043 | 0.020 | 0.044 | 0.048 | 0.017 | 0.044 | 0.048 | 0.077 | 0.331 | 0.340 |
| 3 | 1.062 | 2.235 | 2.475 | 0.098 | 0.074 | 0.122 | 0.491 | 0.585 | 0.764 | 0.092 | 0.035 | 0.099 |
| 4 | 0.027 | 0.038 | 0.047 | 0.023 | 0.051 | 0.056 | 0.125 | 0.244 | 0.275 | 0.256 | 0.441 | 0.510 |
| 5 | 1.311 | 1.376 | 1.901 | 0.031 | 0.332 | 0.333 | 0.039 | 0.317 | 0.319 | 0.069 | 0.433 | 0.438 |
| 6 | 0.349 | 0.631 | 0.721 | 0.041 | 0.041 | 0.058 | 0.409 | 0.734 | 0.840 | 0.165 | 0.078 | 0.183 |
| 7 | 0.026 | 0.045 | 0.052 | 0.050 | 0.053 | 0.073 | 0.203 | 0.199 | 0.284 | 0.026 | 0.042 | 0.049 |
| 8 | 0.020 | 0.041 | 0.046 | 0.023 | 0.039 | 0.045 | 0.559 | 0.333 | 0.650 | 0.068 | 0.656 | 0.660 |
| 9 | 0.125 | 0.132 | 0.181 | 0.013 | 0.059 | 0.060 | 0.316 | 0.335 | 0.461 | 0.239 | 0.184 | 0.302 |
| 10 | 0.405 | 0.544 | 0.679 | 0.036 | 0.075 | 0.084 | 0.025 | 0.063 | 0.068 | 0.029 | 0.058 | 0.065 |
| 11 | 0.102 | 0.151 | 0.182 | 0.080 | 0.156 | 0.175 | 0.591 | 1.002 | 1.163 | 0.789 | 1.237 | 1.467 |
| 12 | N/A | N/A | N/A | N/A | N/A | N/A | 0.966 | 1.139 | 1.494 | 0.174 | 0.294 | 0.342 |
| 13 | N/A | N/A | N/A | 1.851 | 1.261 | 2.240 | 0.365 | 1.536 | 1.578 | 1.080 | 1.202 | 1.616 |
| 14 | 2.662 | 6.291 | 6.831 | N/A | N/A | N/A | 1.330 | 1.047 | 1.693 | 1.147 | 1.764 | 2.104 |
| 15 | 0.016 | 0.041 | 0.044 | 0.024 | 0.044 | 0.050 | 0.013 | 0.037 | 0.040 | 0.077 | 0.273 | 0.284 |
| 16 | 0.028 | 0.048 | 0.056 | 0.020 | 0.044 | 0.049 | 0.016 | 0.042 | 0.045 | 0.080 | 0.299 | 0.310 |
| 17 | 0.155 | 0.171 | 0.231 | 0.017 | 0.042 | 0.045 | 0.018 | 0.042 | 0.046 | 0.076 | 0.303 | 0.312 |
| 18 | 0.011 | 0.044 | 0.046 | 0.016 | 0.041 | 0.044 | 0.011 | 0.046 | 0.047 | 0.077 | 0.314 | 0.323 |
| 19 | 0.020 | 0.037 | 0.042 | 0.019 | 0.035 | 0.040 | 0.015 | 0.038 | 0.041 | 0.103 | 0.345 | 0.360 |
| 20 | 0.048 | 0.037 | 0.060 | 0.018 | 0.035 | 0.040 | 0.019 | 0.034 | 0.039 | 0.082 | 0.325 | 0.335 |
| All | 0.086 | 0.311 | 0.323 | 0.101 | 0.078 | 0.128 | 0.224 | 0.500 | 0.548 | 0.177 | 0.394 | 0.432 |

Table A2. Number of fixed epochs, number of total epochs, and percent of fixed epochs by station and constellation combination.

| | GPS-ONLY | | | GPS+GLO | | | GPS+GAL+BDS | | | GPS+GLO+GAL+BDS | | |
|---|---|---|---|---|---|---|---|---|---|---|---|---|
| Station | n (total) | n (fix) | % fix | n (total) | n (fix) | % fix | n (total) | n (fix) | % fix | n (total) | n (fix) | % fix |
| 1 | 433 | 433 | 100.0 | 480 | 480 | 100.0 | 371 | 371 | 100.0 | 706 | 706 | 100.0 |
| 2 | 435 | 435 | 100.0 | 485 | 485 | 100.0 | 364 | 364 | 100.0 | 677 | 677 | 100.0 |
| 3 | 2158 | 264 | 12.2 | 2525 | 528 | 20.9 | 1814 | 1011 | 55.7 | 2381 | 2007 | 84.3 |
| 4 | 520 | 440 | 84.6 | 483 | 483 | 100.0 | 455 | 455 | 100.0 | 707 | 677 | 95.8 |
| 5 | 2207 | 284 | 12.9 | 2273 | 160 | 7.0 | 1583 | 687 | 43.4 | 2246 | 2215 | 98.6 |
| 6 | 1404 | 299 | 21.3 | 816 | 435 | 53.3 | 1144 | 1061 | 92.7 | 1063 | 855 | 80.4 |
| 7 | 1055 | 429 | 40.7 | 634 | 477 | 75.2 | 711 | 709 | 99.7 | 708 | 708 | 100.0 |
| 8 | 641 | 405 | 63.2 | 483 | 483 | 100.0 | 428 | 428 | 100.0 | 677 | 677 | 100.0 |
| 9 | 582 | 582 | 100.0 | 484 | 484 | 100.0 | 519 | 340 | 65.5 | 738 | 738 | 100.0 |
| 10 | 1696 | 414 | 24.4 | 705 | 541 | 76.7 | 1370 | 1370 | 100.0 | 848 | 819 | 96.6 |
| 11 | 2004 | 244 | 12.2 | 2283 | 399 | 17.5 | 1576 | 1394 | 88.5 | 2534 | 2268 | 89.5 |
| 12 | 942 | 0 | 0.0 | 2457 | 0 | 0.0 | 1726 | 111 | 6.4 | 3755 | 181 | 4.8 |
| 13 | 2393 | 0 | 0.0 | 2526 | 188 | 7.4 | 2231 | 672 | 30.1 | 3711 | 1161 | 31.3 |
| 14 | 2240 | 32 | 1.4 | 2741 | 0 | 0.0 | 2322 | 568 | 24.5 | 4132 | 1491 | 36.1 |
| 15 | 585 | 428 | 73.2 | 453 | 453 | 100.0 | 584 | 552 | 94.5 | 680 | 680 | 100.0 |
| 16 | 615 | 615 | 100.0 | 462 | 462 | 100.0 | 581 | 402 | 69.2 | 589 | 589 | 100.0 |
| 17 | 463 | 463 | 100.0 | 455 | 455 | 100.0 | 434 | 434 | 100.0 | 587 | 587 | 100.0 |
| 18 | 434 | 403 | 92.9 | 452 | 452 | 100.0 | 404 | 404 | 100.0 | 554 | 554 | 100.0 |
| 19 | 443 | 443 | 100.0 | 456 | 456 | 100.0 | 368 | 368 | 100.0 | 596 | 596 | 100.0 |
| 20 | 434 | 431 | 99.3 | 456 | 456 | 100.0 | 395 | 395 | 100.0 | 588 | 588 | 100.0 |
| All | 21684 | 7045 | 32.5 | 22109 | 7958 | 36.0 | 19380 | 12096 | 62.4 | 28477 | 19468 | 68.4 |

Table A3. RMS values by constellation combination, grouped by obstruction category.

| Obstruction | GPS-ONLY | | | GPS+GLO | | | GPS+GAL+BDS | | | GPS+GLO+GAL+BDS | | |
|---|---|---|---|---|---|---|---|---|---|---|---|---|
| | HRMSE (m) | VRMSE (m) | 3DRMSE (m) | HRMSE (m) | VRMSE (m) | 3DRMSE (m) | HRMSE (m) | VRMSE (m) | 3DRMSE (m) | HRMSE (m) | VRMSE (m) | 3DRMSE (m) |
| Low | 0.064 | 0.075 | 0.099 | 0.022 | 0.041 | 0.047 | 0.016 | 0.042 | 0.045 | 0.069 | 0.279 | 0.288 |
| Moderate | 0.134 | 0.226 | 0.263 | 0.031 | 0.048 | 0.058 | 0.328 | 0.449 | 0.556 | 0.171 | 0.341 | 0.382 |
| High | 0.843 | 1.283 | 1.535 | 0.072 | 0.143 | 0.160 | 0.405 | 0.639 | 0.756 | 0.455 | 0.750 | 0.877 |
| Severe | 2.662 | 6.291 | 6.831 | 1.851 | 1.261 | 2.240 | 0.942 | 1.319 | 1.621 | 1.136 | 1.563 | 1.933 |

Table A4. RMS values, standard deviation, and estimated bias by obstruction category.

GPS-ONLY

| Obstruction | n | ERMS (m) | SD E (m) | mean Δe (m) | NRMS (m) | SD N (m) | mean Δn (m) | VRMS (m) | SD Up (m) | mean ΔUp (m) | HRMS (m) | SD H (m) | mean ΔH (m) |
|---|---|---|---|---|---|---|---|---|---|---|---|---|---|
| Low | 3223 | 0.053 | 0.050 | 0.018 | 0.035 | 0.034 | 0.009 | 0.075 | 0.062 | 0.041 | 0.064 | 0.059 | 0.024 |
| Moderate | 2583 | 0.041 | 0.041 | 0.004 | 0.127 | 0.127 | -0.013 | 0.226 | 0.215 | 0.065 | 0.134 | 0.128 | 0.039 |
| High | 1206 | 0.606 | 0.498 | 0.346 | 0.586 | 0.493 | -0.316 | 1.283 | 1.074 | 0.124 | 0.843 | 0.669 | 0.513 |
| Severe | 32 | 1.792 | 0.021 | 1.792 | 1.968 | 0.018 | 1.968 | 6.291 | 0.026 | 6.291 | 2.662 | 0.008 | 2.662 |

GPS+GLO

| Obstruction | n | ERMS (m) | SD E (m) | mean Δe (m) | NRMS (m) | SD N (m) | mean Δn (m) | VRMS (m) | SD Up (m) | mean ΔUp (m) | HRMS (m) | SD H (m) | mean ΔH (m) |
|---|---|---|---|---|---|---|---|---|---|---|---|---|---|
| Low | 3246 | 0.014 | 0.006 | 0.012 | 0.018 | 0.016 | 0.008 | 0.041 | 0.016 | 0.036 | 0.022 | 0.013 | 0.018 |
| Moderate | 2815 | 0.019 | 0.013 | 0.013 | 0.025 | 0.023 | 0.010 | 0.048 | 0.027 | 0.037 | 0.031 | 0.020 | 0.024 |
| High | 1628 | 0.049 | 0.035 | 0.035 | 0.052 | 0.049 | 0.018 | 0.143 | 0.108 | 0.076 | 0.072 | 0.048 | 0.054 |
| Severe | 188 | 0.989 | 0.989 | 0.068 | 1.565 | 1.446 | -0.609 | 1.261 | 0.686 | 1.060 | 1.851 | 0.849 | 1.647 |

GPS+GAL+BDS

| Obstruction | n | ERMS (m) | SD E (m) | mean Δe (m) | NRMS (m) | SD N (m) | mean Δn (m) | VRMS (m) | SD Up (m) | mean ΔUp (m) | HRMS (m) | SD H (m) | mean ΔH (m) |
|---|---|---|---|---|---|---|---|---|---|---|---|---|---|
| Low | 2738 | 0.013 | 0.006 | 0.012 | 0.010 | 0.007 | 0.007 | 0.042 | 0.016 | 0.039 | 0.016 | 0.005 | 0.015 |
| Moderate | 3545 | 0.268 | 0.256 | 0.078 | 0.189 | 0.188 | 0.018 | 0.449 | 0.403 | -0.017 | 0.328 | 0.301 | 0.131 |
| High | 4462 | 0.320 | 0.303 | 0.102 | 0.249 | 0.249 | -0.004 | 0.639 | 0.555 | 0.214 | 0.405 | 0.361 | 0.185 |
| Severe | 1351 | 0.364 | 0.324 | 0.166 | 0.869 | 0.783 | 0.377 | 1.319 | 0.836 | 0.251 | 0.942 | 0.723 | 0.603 |

GPS+GLO+GAL+BDS

| Obstruction | n | ERMS (m) | SD E (m) | mean Δe (m) | NRMS (m) | SD N (m) | mean Δn (m) | VRMS (m) | SD Up (m) | mean ΔUp (m) | HRMS (m) | SD H (m) | mean ΔH (m) |
|---|---|---|---|---|---|---|---|---|---|---|---|---|---|
| Low | 3772 | 0.051 | 0.046 | 0.022 | 0.047 | 0.043 | 0.017 | 0.279 | 0.263 | 0.092 | 0.069 | 0.062 | 0.030 |
| Moderate | 3902 | 0.114 | 0.113 | 0.007 | 0.127 | 0.126 | 0.016 | 0.341 | 0.329 | 0.080 | 0.171 | 0.162 | 0.053 |
| High | 6900 | 0.394 | 0.382 | 0.097 | 0.227 | 0.225 | -0.032 | 0.750 | 0.704 | 0.245 | 0.455 | 0.438 | 0.121 |
| Severe | 2518 | 0.587 | 0.534 | 0.243 | 0.973 | 0.856 | -0.463 | 1.563 | 1.040 | 0.629 | 1.136 | 0.979 | 0.577 |

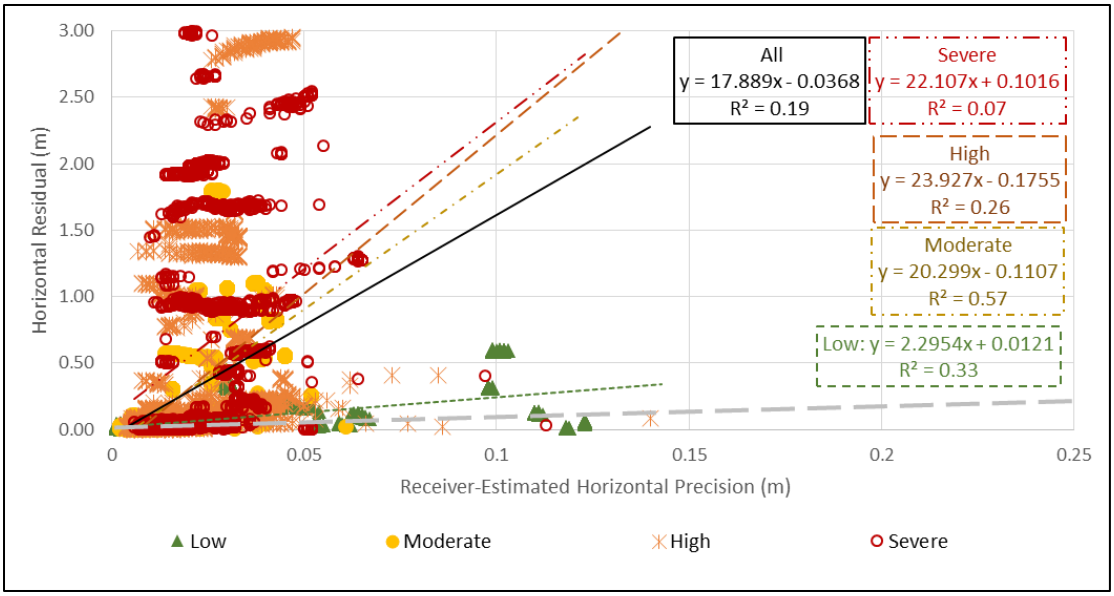


Figure A1. Computed horizontal residual versus receiver-estimated horizontal precision, grouped by obstruction category.

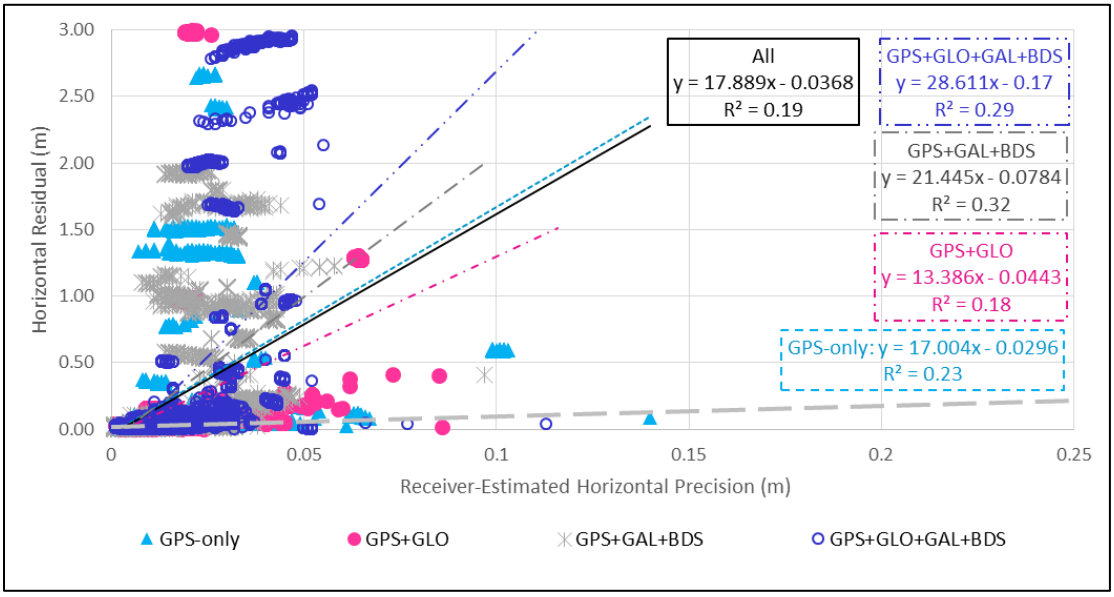


Figure A2. Computed horizontal residual versus receiver-estimated horizontal precision, grouped by constellation combination.